Prediction Of Worldwide Energy Resource (POWER)
--- Agroclimatology Methodology ---
(1.0^{o} Latitude by 1.0^{o} Longitude Spatial Resolution)

(Version 1.0.2 June 4, 2015)

Paul W. Stackhouse, Jr[1], David Westberg[2], James M. Hoell[2],
William S. Chandler[2], Taiping Zhang[2]
[1]NASA Langley Research Center [2]SSAI/NASA Langley Research Center

I. Introduction

NASA, through its' Earth science research program has long supported satellite systems and research providing data important to the study of climate and climate processes. These data include long-term estimates of meteorological quantities and surface solar energy fluxes. These satellite and modeled based products have also been shown to be accurate enough to provide reliable solar and meteorological resource data over regions where surface measurements are sparse or nonexistent, and offer two unique features – the data is global and, in general, contiguous in time. These two important characteristics, however, tend to generate very large data files/archives which can be intimidating for users, particularly those with little experience or resources to explore these large data sets. Moreover, the data products contained in the various NASA archives are often in formats that present challenges to new users. NASA's Applied Sciences Program (http://appliedsciences.nasa.gov/about.php) was established to foster the use of Earth science research results for near-term applications and benefits. The Prediction Of Worldwide Energy Resource (POWER) project is one of the activities funded by the Applied Science Program.

The POWER project was initiated in 2003 as an outgrowth of the Surface meteorology and Solar Energy (SSE - https://eosweb.larc.nasa.gov/project/sse/sse_table) project. The SSE project has as its focus the development of parameters related to the solar based energy industry. The current POWER project encompasses the SSE project with the objective to improve subsequent releases of SSE, and to create new datasets with applicability to the architectural (e.g. Sustainable buildings) and agricultural (e.g. Agro-climatology) industries. The POWER web interface (http://power.larc.nasa.gov) currently provides a portal to the SSE data archive, tailored for the renewable energy industry, as well as to the Sustainable Buildings Archive with parameters tailored for the sustainable buildings community, and the Agroclimatology Archive with parameters for the agricultural industry. In general, the underlying data behind the parameters used by each of these industries is the same – global solar radiation, or insolation, and meteorology, including surface and air temperatures, moisture, and winds.

The purpose of this document is to describe the underlying data contained in the Agroclimatology Archive, and to provide additional information relative to the various industry specific parameters, their limitations, and estimated accuracies. The intent is to provide information that will enable new and/or long time users to make decisions concerning the suitability of the Agroclimatology data for their project in a particular region of the globe. This document is focused primarily on the Agroclimatology parameters, although the underlying solar and meteorological data for all three POWER archives (SSE, Sustainable Buildings, and Agroclimatology) are the derived from common data sources.

Companion documents describe the data and parameters in the POWER/SSE and POWER/ Sustainable Buildings sections of the POWER data portal.

(Return to Content)

II. Agroclimatology Archive: Parameters & Data Sources:

The parameters contained in the Agroclimatology Archive are based primarily upon solar radiation derived from satellite observations and meteorological data from assimilation models. The various parameters have been selected and developed through close collaboration with industry and government partners in the agricultural community, and a web-based portal provides access to industry-friendly parameters.

The archive contains (1) daily solar insolation data from July 1, 1983 to within seven days of present time; (2) daily values of the minimum, maximum and averaged temperatures from January 1, 1983 to within 3 days of current time; (3) daily precipitation from January 1, 1997 – August 31, 2009; and (4) daily wind speed from January 1, 1983 – to within 3 days of current time. All parameters are available globally as time series data for any user specified latitude, longitude. The spatial resolution of all parameters is 1 – degree of latitude and longitude.

Parameters in the Agroclimatology Archive have been developed from various data sources as follows:

(1) For the time period July 1, 1983 – December 31, 2007 solar parameters are taken from release 3 of the NASA/GEWEX Surface Radiation Budget (GEWEX SRB 3.0 - https://eosweb.larc.nasa.gov/project/srb/srb_table;

(2) For the time period from January 1, 2008 to within a week of real time solar parameters from NASA's Fast Longwave And SHortwave Radiative Fluxes (FLASHFlux - http://flashflux.larc.nasa.gov/) project

(3) Meteorological parameters (e.g. temperature, relative humidity, and dew point) are from NASA's Global Model and Assimilation Office (GMAO - http://gmao.gsfc.nasa.gov/), Goddard Earth Observing System model version 4 (GEOS-4) for the time period from January 1, 1983 – December 31, 2007; and from GEOS-5 for the time period from January 1, 2008 to within several days of real time.

(4) Daily precipitation values are from the Global Precipitation Climate Project (GPCP - http://precip.gsfc.nasa.gov/) currently from January 1987 - August 2009.

(5) Daily m wind data is based upon the NASA/GMAO GEOS version 4 (GEOS-4) for the time period January 1 1983 – December 31, 2007; GEOS-5 for time period January 1, 2008 to within several days of real time.

Table II-1 gives a more detailed overview of the parameters, the respective temporal coverage, and various programs from which the underlying solar and meteorological data are obtained.

Note that the time series of daily surface insolation is comprised of values from the GEWEX SRB project (July 1983 – December 31 2007) and the FLASHFlux project (January 1, 2008 – near real time); and daily temperature data is comprised of results from the GEOS-4 assimilation model (January 1, 1983 – December 31, 2007) and the GEOS-5 assimilation model (January 1,

2008 to within several days of current time). Care should be taken when assessing climate trends that encompass the pre- and post-January 1, 2008 data.

Table II-1. THE POWER – AGROCLIMATOLOGY ARCHIVE: PARAMETERS, TEMPORAL COVERAGE & DATA SOURCES

DAILY INSOLATION:
(July 1, 1983 - December 31, 2007 →GEWEX SRB 3.0;
January 1, 2008 - Near present → FLASHFlux)

- Top-of-atmosphere Insolation
- Shortwave Insolation on Horizontal Surface
- Downward Longwave Radiative Flux

DAILY METOROLOGICAL:
(**January 1, 1983 - December 31, 2007 →GEOS-4;**
January 1, 2008 - Near present → GEOS -5)

- Average Air Temperature at 2 m
- Minimum Air Temperature at 2 m
- Maximum Air Temperature at 2 m
- Relative Humidity at 2 m
- Dew/Frost Point Temperature at 2 m

DAILY PRECIPITATION:
(**January 1, 1997 - August 31, 2009 → GPCP 1-degree daily)**

DAILY WIND SPEED AT 10M:
(January 1, 1983 - December 31, 2007 → GEOS-4;
January 1, 2008 - Near present → GEOS-5)

(Return to Content)

III. Parameter Accuracy-Summary:

This section provides a summary of the estimated uncertainty associated with the solar and meteorological data available through the POWER/Agroclimatology archive. The uncertainty estimates are based upon comparisons with ground measurements. A more detailed description of the parameters and the procedures used to estimate their uncertainties is given in the subsequent sections of this document. Additional validation studies have been reported by White, et al. (2008 and 2011) and by Bai, et al (2010).

(Return to Content)

III-A. Solar Insolation: Quality ground-measured data are generally considered more accurate than satellite-derived values. However, measurement uncertainties from calibration drift, operational uncertainties, or data gaps are often unknown or unreported for many ground site data sets. In 1989, the World Climate Research Program estimated that most routine-operation solar-radiation ground sites had "end-to-end" uncertainties from 6 to 12%. Specialized high quality research sites such as those in the Baseline Surface Radiation Network (BSRN -

http://www.bsrn.awi.de/en/home/ ; Ohmura *et al*., 1999) are estimated to be more accurate by a factor of two.

Table III-A.1 summarizes the results of comparing respectively the daily NASA/GEWEX SRB 3.0 and FLASHFlux solar shortwave insolation on a horizontal surface to observations from the BSRN. The GEWEX/SRB 3.0 values are compared to BSRN observations (see Figure IV-2 for location of BSRN stations) for the time period January 1, 1992, the beginning of the BSRN observations, through December 31, 2007. The FLASHFlux values are compared to BSRN observation for the time period January 1, 2008 – December 31, 2010.

Table III-A.1. Bias and Root Mean Square Error (RMSE) associated with comparison of GEWEX SRB 3.0 and FLASHFlux Shortwave (SW) and Longwave (LW) Insolation on a horizontal surface to BSRN observational values.

Parameter	Region	Bias (%)	RMSE (%)
GEWEX SRB 3.0 Daily SW Insolation (Jan 1992 – Dec 2007) Figure IV-3	Global 60° Poleward 60° Equatorward	-1.80 -7.70 -1.14	20.21 41.32 17.65
FLASHFlux Daily SW Insolation (Jan 2008 – Dec 2010) Figure IV-4	Global 60° Poleward 60° Equatorward	-2.83 -11.82 -1.61	18.35 35.41 15.08
GEWEX SRB 3.0 Daily LW Insolation (Jan 1992 – Dec 2007) Figure IV-5	Global 60° Poleward 60° Equatorward	0.16 1.27 -0.03	7.0 13.44 5.73
FLASHFlux Daily LW Insolation (Jan 2008 – Dec 2010) Figure IV-6	Global 60° Poleward 60° Equatorward	-0.25 4.16 -1.09	6.20 12.14 5.14

(Return to Content)

III.B Meteorology: This section provides a summary of the estimated uncertainty associated with the meteorological data available through the POWER/Agroclimatological archive. As with the solar validations, the uncertainty estimates are based upon comparisons with ground measurements. A more detailed description of the parameters and the procedures used to estimate their uncertainties is given in the subsequent sections of this document.

Table III-B.1 summarize the results of comparing GEOS-4 meteorological parameters to ground observations reported in the National Climatic Data Center (NCEI) global summary of the day (GSOD) files. Table III-B.2 summarizes the comparison statistics for the GEOS-4 and GEOS-5 wind speed comparisons. Table III-B.3 summarizes the comparison statistics associated with daily GPCP precipitation values.

Table III-B.1: Linear least squares regression parameters associated with scatter plots of uncorrected GEOS-4 meteorological values versus ground observations over the time period January 1983 through December 31, 2006. (See Appendix A for a discussion of a downscaling methodology which can improve the agreement between assimilation model estimates of temperatures and ground site observations.)

Parameter	Slope	Intercept	R^2	RMSE	Bias
Tmax (°C) (Table V-A.1a)	0.96	-1.16	0.91	3.95	-1.82
Tmin (°C) (Table V-A.1b)	0.99	0.32	0.91	3.46	0.26
Tavg (°C) (Table V-A.1c)	1.00	-0.57	0.94	2.75	-0.56
Tdew (°C)	0.96	-0.80	0.95	2.46	-1.07
RH (%)	0.79	12.72	0.56	9.40	-1.92
Surface Atmospheric Pressure (hPa)	0.89	102.16	0.74	27.33	-10.20

Table III-B.2: Regression parameters associated with scatter plots of the daily averaged GEOS wind speeds versus ground observations for the indicated time period.

Parameter	Slope	Intercept (m^2)	R^2	RMSE (m^2)	Bias (m^2)
GEOS-4 Wind Speed at 10 meters (Jan. 1, 2007 – Dec. 31, 2007)	0.55	1.62	0.42	1.76	0.011
GEOS-5 Wind Speed at 10 meters (m/s) (Jan. 1, 2009 – Dec. 31, 209)	0.65	1.62	0.46	1.83	0.38

Table III-B.3 summarizes the regression parameters associated with scatter plots of the GPCP 1-DD daily precipitation values versus ground observations reported in the NCEI GSOD files for the continental US

Table III-B.3: Linear least squares regression parameters associated with scatter plots of GPCP daily 1-degree spatial precipitation estimates verses ground observations.

Parameter	Slope	Intercept (mm)	R^2	RMSE\ (mm)	Bias \(mm)
Daily 1-DD GPCP precipitation	0.42	1.78	0.22	7.02	0.68
Monthly Average of Daily GPCP	0.60	1.43	0.46	1.72	0.68

(Return to Content)

IV. Global Insolation on a Horizontal Surface:

The daily solar radiation values for the time period July 1983 – December 2007 are obtained from the NASA/Global Energy and Water Cycle Experiment - Surface Radiation Budget Project Release 3.0 archive (NASA/GEWEX SRB 3.0; see http://gewex-srb.larc.nasa.gov/ & https://eosweb.larc.nasa.gov/project/srb/srb_table). Daily Solar radiation values for the time period from January 1, 2008 to within a week of real time are obtained from NASA's Fast Longwave And SHortwave Radiative Fluxes (FLASHFlux; see http://flashflux.larc.nasa.gov/) project.

The NASA/GEWEX SRB Project focuses on providing climatological estimates of the Earth's Top-of-atmosphere (TOA) and surface radiative energy flux components in support of NASA's effort to quantify components of the Earth's radiation budget, while the focus of the FLASHFlux project is to provide solar data within one week of satellite observations.

While it is not the intent or purpose of this document to provide a detailed description of the methodology for inferring solar data from satellite observations, a brief synopsis is provided in the following sections.

(Return to Content)

IV.A. Earth's Radiation budget: A central focus of the NASA's satellite programs is to quantify the process associated with the Earth's energy budget. Figure IV.1 illustrates the major components/processes associated with the Earth's Energy Budget including updated radiative flux components estimated from SRB Release 3.0 in the yellow boxes. These values are based on a 24 year (July 1983 – Dec. 2007) annual global averaged radiative fluxes with year-to-year annual average variability of +/- 4 W m^{-2} in the solar wavelengths and +/- 2 W m^{-2} in the thermal infrared (longwave) flux estimates. The absolute uncertainty of these components is still the

subject of active research. For instances, the most recent satellite based measurements of the incoming solar radiation disagree with previous measurements and indicate this value should be closer 340.3 W m^{-2} providing another source of uncertainty. Other uncertainties involving the calibration of satellite radiances, atmospheric properties of clouds, aerosols and gaseous constituents, surface spectral albedos are all the subject of research within the GEWEX SRB project.

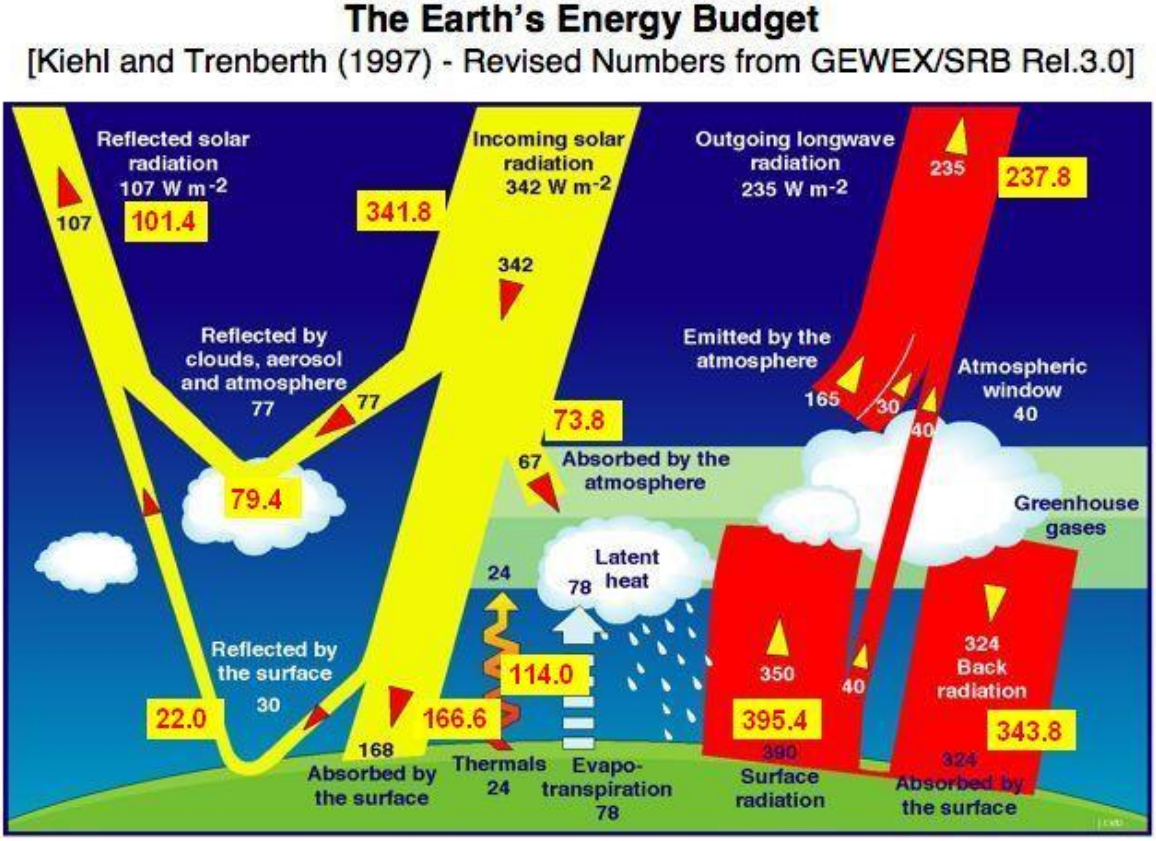

Figure IV-1. The major components/processes associated with the Earth's Energy Budget. The values in the yellow rectangles are based upon the updated solar and thermal infrared radiation estimates in SRB Release 3.0. (Note that all units are in W/m^2; multiplying W/m^2 by 0.024 yields kWh/day/m^2, and by 0.0864 yields MJ/day/m^2.)

(Return to Content)

IV-B Radiative Transfer Model:

IV-B.i. GEWEX SRB Radiative Transfer Model: The process of inferring the surface solar radiation, or insolation, from satellite observations employs the modified method of Pinker and Laszlo (1992). This method involves the use of a radiative transfer model, along with water vapor column amounts from the GEOS-4 product and ozone column amounts from satellite measurements. Three satellite visible radiances are used: the instantaneous clear sky radiance,

the instantaneous cloudy sky radiance, and the clear sky composite radiance, which is a representation of a recent dark background value. The observed satellite radiances are converted into broadband shortwave TOA albedos, using Angular Distribution Models from the Earth Radiation Budget Experiment (Smith et al., 1986). The spectral shape of the surface albedo is fixed by surface type. The radiative transfer model (through the use of lookup tables) is then used to find the absolute value of the surface albedo which produces a TOA upward flux which matches the TOA flux from the conversion of the clear-sky composite radiance. For this step, a first guess of the aerosol amount is used. The aerosol used for this purpose was derived from six years (2000-2005) of daily output from the MATCH chemical transport model (Rasch *et al.*,1997). A climatology of aerosol optical depth was developed for each of the twelve months by collecting the daily data for each grid cell, and finding the mode of the frequency distribution. The mode was used rather than the average so as to provide a typical background value of the aerosol, rather than an average which includes much higher episodic outbreak values. The surface albedo now being fixed, the aerosol optical depth is chosen within the radiative transfer model to produce a TOA flux which matches the TOA Flux from the conversion of the instantaneous clear sky radiance. Similarly the cloud optical depth is chosen to match the TOA flux implied from the instantaneous cloudy sky radiance. With all parameters now fixed, the model outputs a range of parameters including surface and TOA fluxes. All NASA/GEWEX SRB 3.0 parameters are output on a 1^0 by 1^0 global grid at 3-hourly temporal resolution for each day of the month.

Primary inputs to the model include: visible and infrared radiances, and cloud and surface properties inferred from International Satellite Cloud Climatology Project (ISCCP) pixel-level (DX) data (Rossow and Schiffer, 1999; data sets and additional information can be found at https://eosweb.larc.nasa.gov/project/isccp/isccp_table); temperature and moisture profiles from GEOS-4 reanalysis product obtained from the NASA Global Modeling and Assimilation Office (GMAO; Bloom et al., 2005); and column ozone amounts constituted from Total Ozone Mapping Spectrometer (TOMS) and TIROS Operational Vertical Sounder (TOVS) archives, and Stratospheric Monitoring-group's Ozone Blended Analysis (SMOBA), an assimilation product from NOAA's Climate Prediction Center.

To facilitate access to the GEWEX SRB 3.0 data products, the POWER project extracts the fundamental parameters (i.e. solar) from the SRB archive and metrological from the GEOS-4 & 5.1 and GPCP archives. The data products listed in Table III are available through the respective archives although in some instances the product may be bundled with a number of other parameters and generally are large global spatial files (i.e. 1 per day) rather than temporal files.

(Return to Content)

IV-B.ii. FLASHFlux Radiative Transfer Model: The Fast Longwave and SHortwave Flux (FLASHFlux) project is based upon the algorithms developed for analysis and data collected by the Clouds and the Earth's Radiant Energy System (CERES - http://ceres.larc.nasa.gov/) project. CERES is currently producing world-class climate data products derived from measurements taken aboard NASA's Terra and Aqua spacecrafts. While of exceptional fidelity, CERES data products require a extensive calibration checks and validation to assure quality and verify accuracy and precision. The result is that CERES data are typically released more than six

months after acquisition of the initial measurements. For climate studies, such delays are of little consequence especially considering the improved quality of the released data products. There are, however, many uses for the CERES data products on a near real-time basis such as those referred to within the POWER project. To meet those needs, FLASHFlux has greatly speeded up the processing by using the earliest stream of data coming from CERES instruments and using fast radiation algorithms to produce results within one week of satellite observations. This results in the loss of climate-quality accuracy due to bypassing of some calibration checks, and some gaps in the earliest stream of satellite data.

For speedy retrieval of surface insolation, FLASHFlux uses the SW Model B that is also used in CERES processing. This model is named the Langley Parameterized SW Algorithm (LPSA) and described in detail in Gupta et al. (2001). It consists of physical parameterizations which account for the attenuation of solar radiation in simple terms separately for clear atmosphere and clouds. Surface insolation, F_{sd}, is computed as

$$F_{sd} = F_{toa}\ T_a\ T_c\ ,$$

where F_{toa} is the corresponding TOA insolation, T_a is the transmittance of the clear atmosphere, and T_c is the transmittance of the clouds. Both FLASHFlux and CERES rely on similar input data sets from the meteorological products and MODIS. However, it is important to note that even though the FLASHFlux endeavor intends to incorporate the latest input data sets and improvements into its algorithms, there are no plans to reprocess the FLASHFlux data products once these modifications are in place. Thus, in contrast to the CERES data products, the FLASHFlux data products are **not** to be considered of climate quality. Users seeking climate quality should instead use the CERES data products. In the following section estimates of the accuracy of the GEWEX SRB 3.0 and FLASHFlux solar data are provided.

(Return to Content)

IV.C. Validation: The solar data in the GEWEX SRB 3.0 (July 1983 – December 2007) and FLASHFlux (January 2008 – near real time) data have been tested/validation against research quality observation from the Baseline Surface Radiation Network (BSRN; Ohmura *et al*., 1999). Figure IV-2 shows the location of ground stations within the BSRN networks/archives.

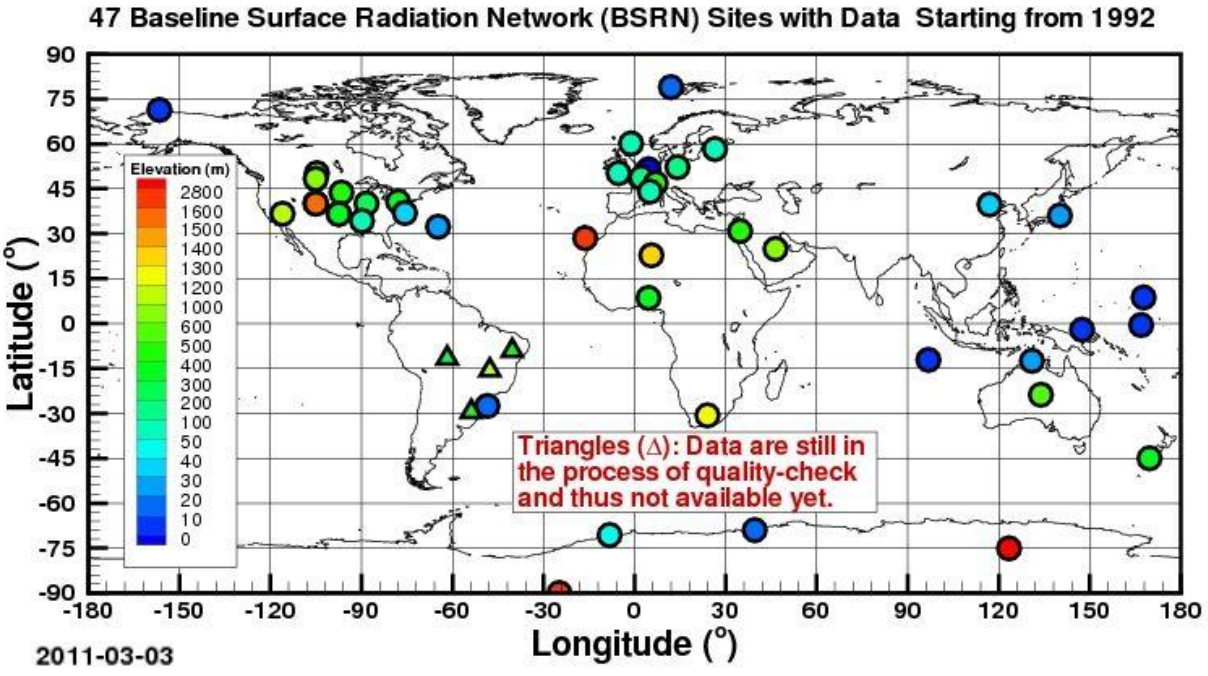

Figure IV-2. Location of ground stations in the Baseline Surface Radiation Network (BSRN).

(Return to Content)

IV.C-i. Daily Mean Shortwave Insolation: Scatter plots of the total (i.e. diffuse plus direct) daily mean surface insolation observed at the BSRN ground sites versus insolation values from the SRB release 3.0 are shown Figure IV-3. The time period is from January 1, 1992, the earliest that data from BSRN is available, through December 31, 2007. In Figure IV-4 a similar scatter plot for daily mean FLASHFlux values is shown with the time period from January 1, 2008 – December 31, 2010.

Correlation and accuracy parameters for each scatter plots are given in the legend box in each figure. Note that the correlation and accuracy parameters are given for all sites (e.g. Global), for the BSRN sites in regions above 60^o latitude, north and south (i.e. 60^0 poleward), and for BSRN sites between 60^o north and 60^o south (i.e. 60^o equatorward). The Bias is the difference between the mean (μ) of the respective solar radiation values for SRB and BSRN. The RMS is the root mean square difference between the respective SRB and BSRN values. The correlation coefficient between the SRB and BSRN values is given by ρ, the variance in the SRB values is given by σ, and N is number of SRB:BSRN pairs for each latitude region.

We note here that 3-hourly SRB values are the initial values estimated through the retrieval process described in Section IV-B.i and are used to calculate the daily total insolation shown in Figure IV-3. The 3-hourly values are available through the Atmospheric Science Data Center (ASDC/SRB – https://eosweb.larc.nasa.gov/project/srb/srb_table).

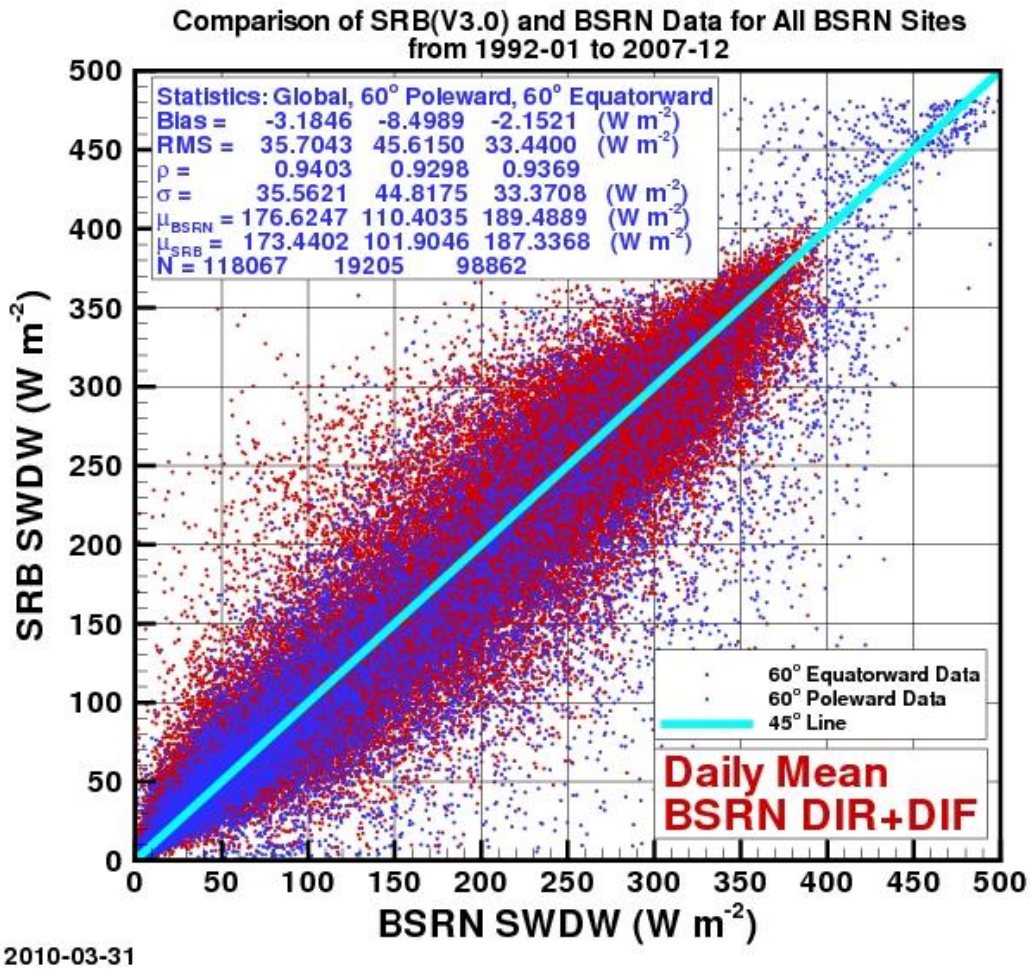

Figure IV-3. Scatter plot of daily total surface solar radiation observed at BSRN ground sites over the years 1992 - 2007 versus daily values from the GEWEX/SRB Release 3.0 archive all sky conditions. These daily are used to calculate the monthly averages that are provided in POWER/Agroclimatology Archive. (Note that solar radiation is in W/m^2; multiplying W/m^2 by 0.024 yield KWh/m^2/day and by 0.0864 yields MJ/day/m^2.)

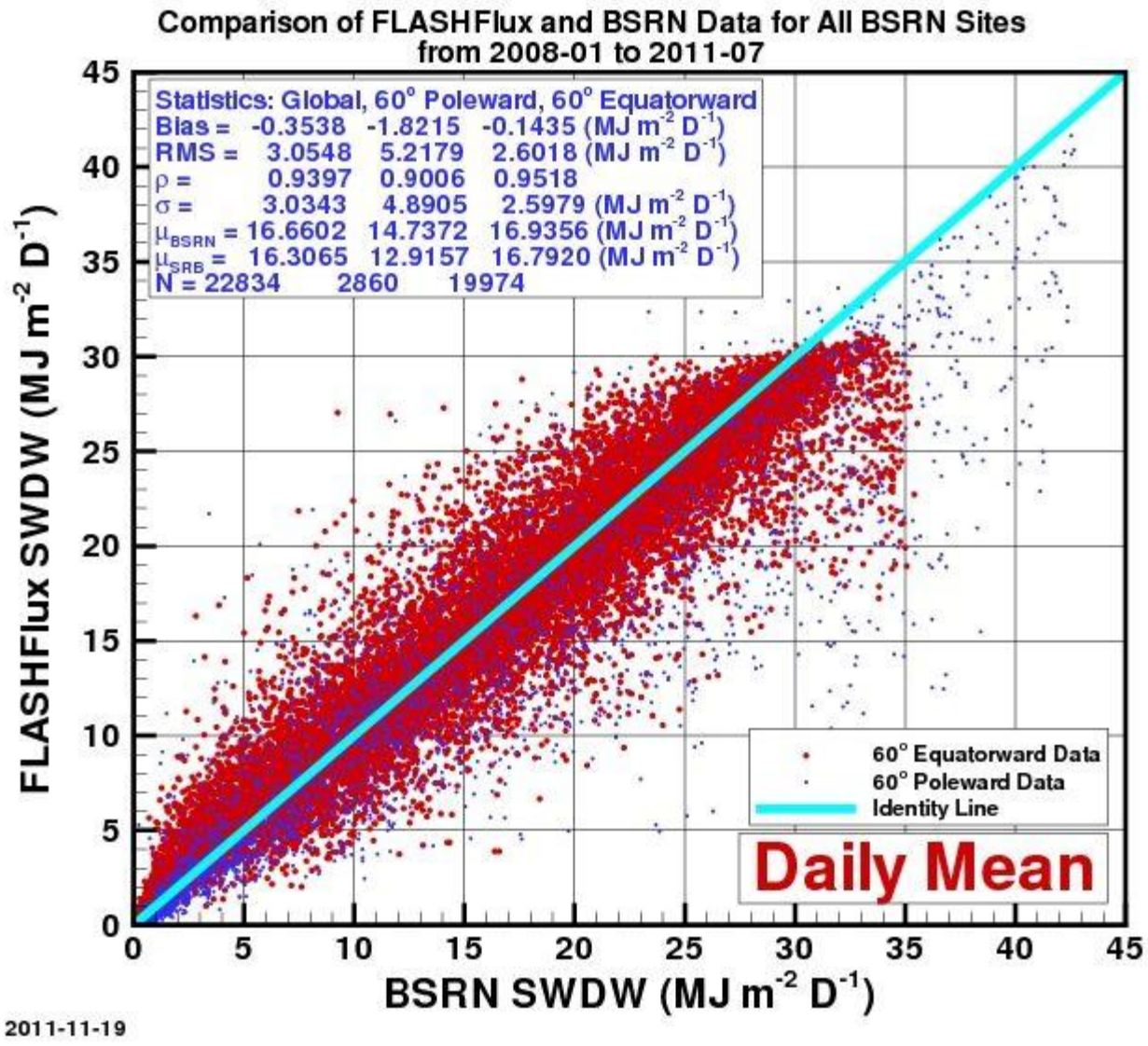

Figure IV-4. Scatter plot of daily total surface solar shortwave radiation observed at BSRN ground sites over the years 2008 - 2011 versus daily values from the FLASHFlux archive. (Note that solar radiation is in MJ/day/m^2; multiplying MJ/day/m^2 by 0.2778 yield KWh/m^2/day and by 11.574 yields w/m^2.)

(Return to Content)

IV.C-ii. Daily Mean Longwave Insolation:

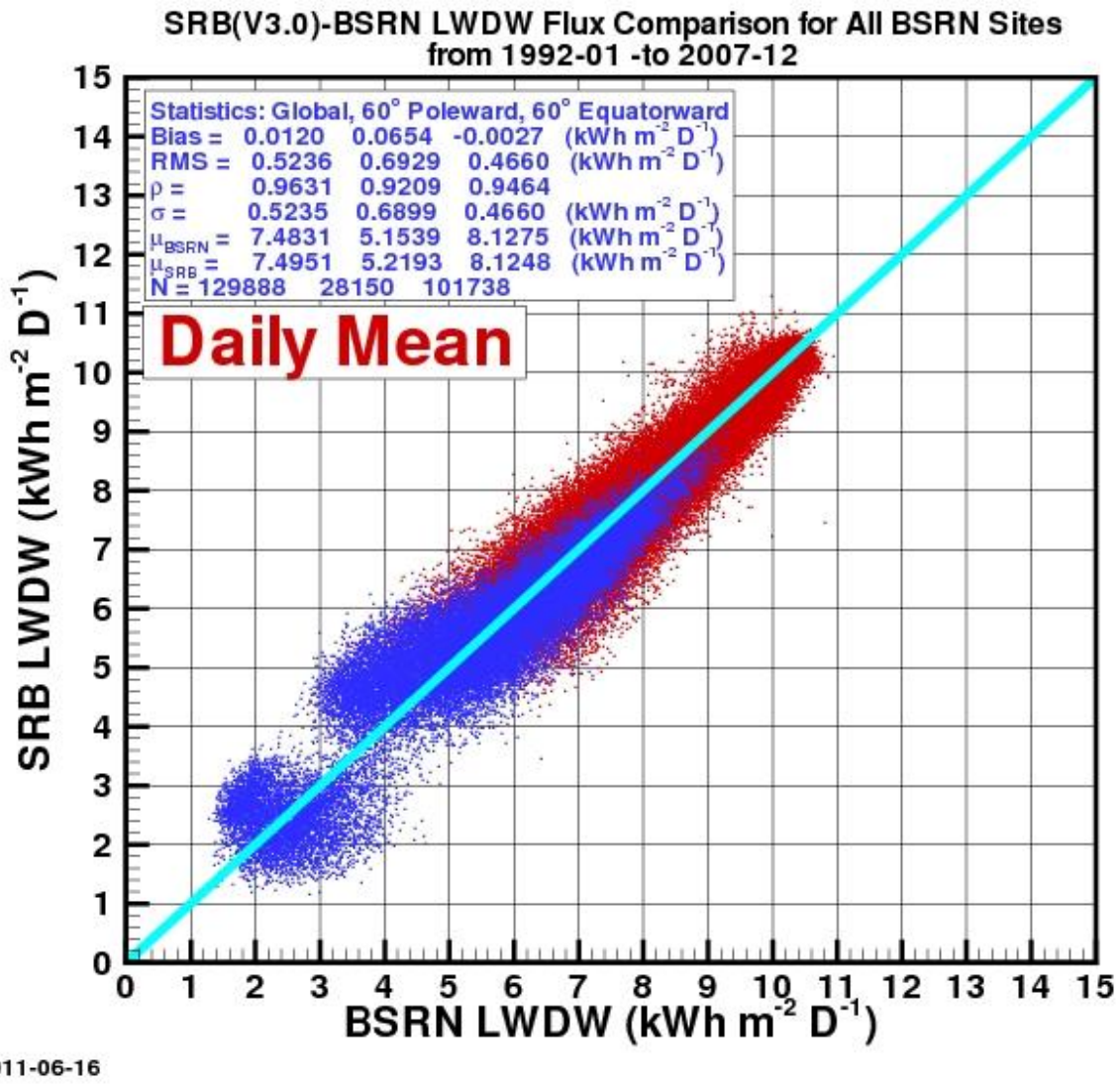

Figure IV-5. Scatter plot of daily mean total surface solar longwave insolation observed at BSRN ground sites over the years 1992 - 2007 versus daily means from the SRB Project for all sky conditions. (Note that solar radiation is in KWh/m^2/day; multiplying KWh/m^2/day by 41.67 yields W/m^2; and by 3.6 yields MJ/day/m^2.)

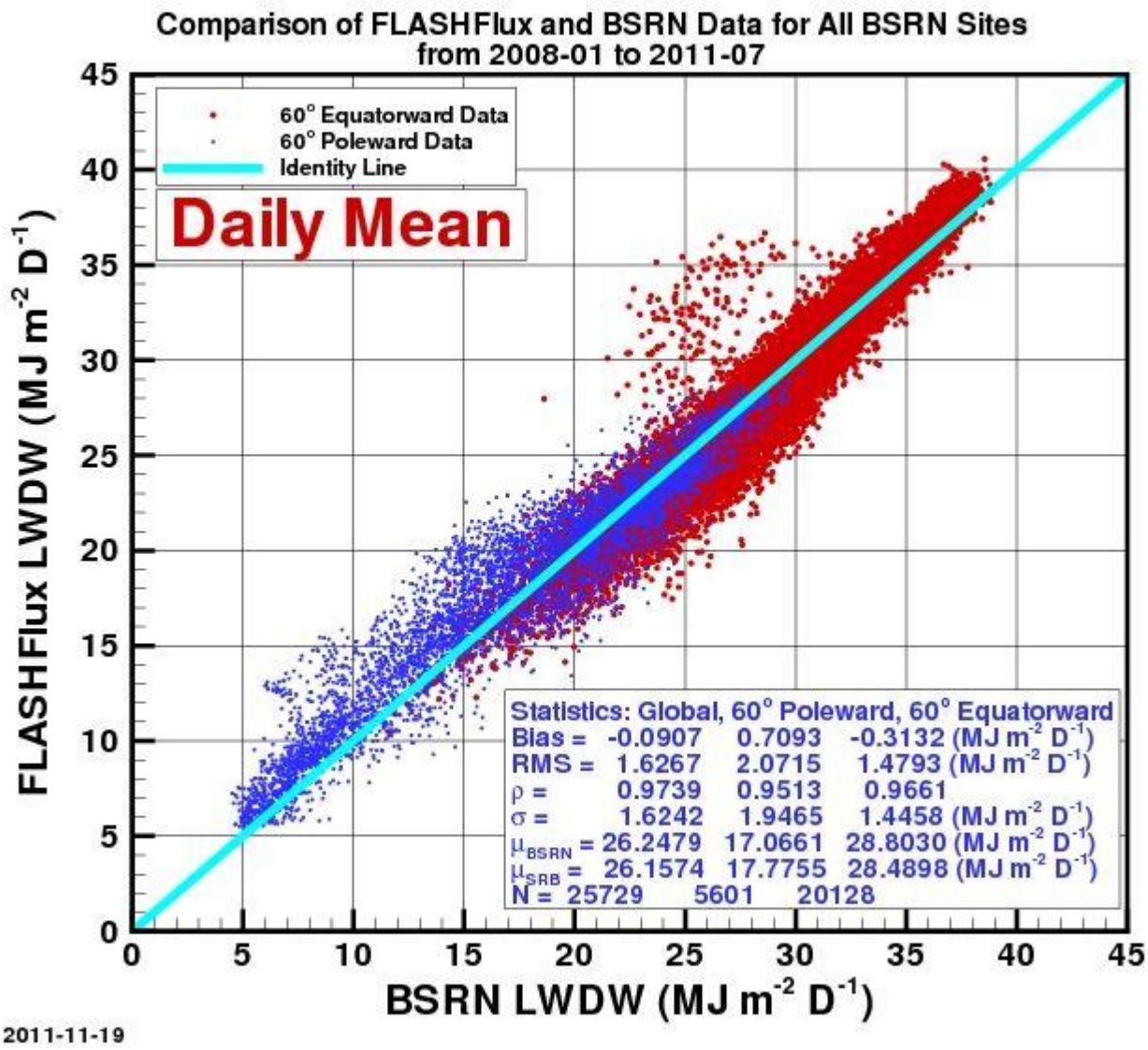

Figure IV-6. Scatter plot of daily mean total surface solar longwave insolation observed at BSRN ground sites over the years 2008 - 2010 versus daily means from the FLASHflux Project for all sky conditions. (Note that solar radiation is in KWh/m^2/day; multiplying KWh/m^2/day by 41.67 yields W/m^2; and by 3.6 yields MJ/day/m^2.)

(Return to Content)

V. Meteorological Parameters

Table II-1 lists the meteorological parameters provided through the Agroclimatology archive, their temporal coverage and source. The global distribution of temperature parameters in the POWER/Agroclimatology archive are obtained from NASA's Global Model and Assimilation Office (GMAO), Goddard Earth Observing System global assimilation models version 4 (GEOS-

4: http://gmao.gsfc.nasa.gov/systems/geos4/) and version-5 (GEOS-5: http://gmao.gsfc.nasa.gov/products/) . The relative humidity is a calculated parameter based upon pressure, temperature and specific humidity, all parameters obtained from the assimilation models. Dew/frost point temperatures are calculated values based upon the relative humidity and air temperature which is obtained from the assimilation model. Precipitation is obtained from the GPCP 1-DD Satellite-Gauge product. Daily wind speeds are from the GEOS-4 assimilation model over the time period January 1, 1983 – December 31, 2007 and from the GEOS-5 model over the time period January 1, 2008 – to within several days of current time. In this section the results associated with testing /validating each parameter against ground site observation is discussed.

(Return to Content)

V.A. Assessment GEOS-4 Assimilation Model Global Temperatures: As noted above all meteorological parameters, except precipitation, are based directly or indirectly (i.e. calculated) on the GMAO assimilation models. The meteorological parameters emerging from the GMAO assimilation models are estimated via "An atmospheric analysis performed within a data assimilation context [that] seeks to combine in some "optimal" fashion the information from irregularly distributed atmospheric observations with a model state obtained from a forecast initialized from a previous analysis." (Bloom, et al., 2005). The model seeks to assimilate and optimize observational data and model estimates of atmospheric variables. Types of observations used in the analysis include (1) land surface observations of surface pressure; (2) ocean surface observations of sea level pressure and winds; (3) sea level winds inferred from backscatter returns from space-borne radars; (4) conventional upper-air data from rawinsondes (e.g., height, temperature, wind and moisture); (5) additional sources of upper-air data include drop sondes, pilot balloons, and aircraft winds; and (6) remotely sensed information from satellites (e.g., height and moisture profiles, total perceptible water, and single level cloud motion vector winds obtained from geostationary satellite images). Emerging from the analysis are 3-hourly global estimates of the vertical distribution of a range of atmospheric parameters. The assimilation model products are bi-linearly interpolated to a 1^0 by 1^0 grid.

In addition to the analysis reported by the NASA's Global Model and Assimilation Office (GMAO) (Bloom, et al.), the POWER project initiated a study focused on determining the accuracy of the modeled meteorological parameters in terms of the applications within the POWER project. In particular, the temperatures (minimum, maximum and daily averaged air and dew point), relative humidity, and winds have been explicitly compared to global data obtained from the National Center for Environmental Information (NCEI – formally National Climatic Data Center http://www.ncdc.noaa.gov/oa/ncdc.html) global "Summary of the Day" (GSOD) files, and to observations from other high quality networks such as the Surface Radiation (SURFRAD - http://www.srrb.noaa.gov/surfrad/index.html), Atmospheric Radiation Measurement (ARM - http://www.arm.gov/), as well as observations from automated weather data networks such as the High Plains Regional Climate Center (HPRCC - http://www.hprcc.unl.edu/index.php).

In this section we will focus primarily on the analysis of the GEOS-4 daily maximum and minimum temperatures, and the daily mean temperature using observations reported in the NCEI

- GSOD files, with only summary comments regarding results from the other observational networks noted above. The GEOS-4 re-analysis model outputs meteorological parameters at 3-hourly increments (e.g. 0, 3, 6, 9, 12, 15, 18, and 21 Z) on a global 1- deg by 1.25-deg grid at 50 pressure levels. The 1-deg by 1.25-deg grid is bi-linearly interpolated to a 1-deg by 1-deg grid to match the GEWEX/SRB 3.0 solar radiation values. The local daily maximum (Tmax) and minimum (Tmin) temperature, and the local daily mean (Tave) temperature at 2 meters above the surface were obtained from the GEOS-4 3-hourly data. The Agroclimatology GEOS-4 meteorological data spans the time period from January 1, 1983 - through December 2007; comparative analysis discussed here is based upon observational data from January 1, 1983 through December 31, 2006.

The observational data reported in the NCEI GSOD files are hourly observations from globally distributed ground stations with observations typically beginning at 0Z. For the analysis reported herein, the daily Tmin, Tmax and Tave were derived from the hourly observations filtered by an "85%" selection criteria applied to the observations reported for each station. Namely, only data from NCEI stations reporting 85% or greater of the possible 1-hourly observations per day and 85% or greater of the possible days per month were used to determine the daily Tmin, Tmax, and Tave included in comparisons with the GEOS-4 derived data. Figure V-A.1 illustrates the global distribution of the surface stations remaining in the NCEI data files for 1983 and 2004 after applying our 85% selection criteria. Note that the number of stations more than doubled from 1983 (e.g. 1104 stations) to 2004 (e.g. 2704 stations), and that majority of the stations are located in the northern hemisphere.

Unless specifically noted otherwise, all GEOS-4 air temperatures represent the average value on a 1^o x 1^o latitude, longitude grid cell at an elevation of 2 m above the earth's surface and NCEI values are ground observations at an elevation of 2 meters above the earth's surface. Scatter plots of Tave, Tmax, and Tmin derived from ground observations in the NCEI files versus GEOS-4 values for the years 1987 and 2004 are shown in Figure V-A.2. These plots illustrate the agreement typically observed for all the years 1983 through 2006. In the upper left corner of each figure are the parameters for the linear least squares regression fit to theses data, along with the mean Bias and RMSE between the GEOS-4 and NCEI observations. The mean Bias and RMSE are given as:

$$\text{Bias} = \sum_j \{\sum_i \{[(T_i^j)_{GEOS4} - (T_i^j)_{NCEI}]\}\}/N$$

$$\text{RMSE} = \{\sum_j \{\sum_i \{[(T_i^j)_{GEOS4} - (T_i^j)_{NCEI}]^2/N\}\}\}^{1/2},$$

where, $\sum_i$ is summation over all days meeting the 85% selection criteria, $\sum_j$ indicates the sum over all stations, $(T_i^j)_{NCEI}$ is the temperature on day i for station j, and $(T_i^j)_{GEOS4}$ is the GEOS-4 temperature corresponding to the overlapping GEOS-4 1-degree cell for day i and station j, and N is the number of matching pairs of NCEI and GEOS-4 values.

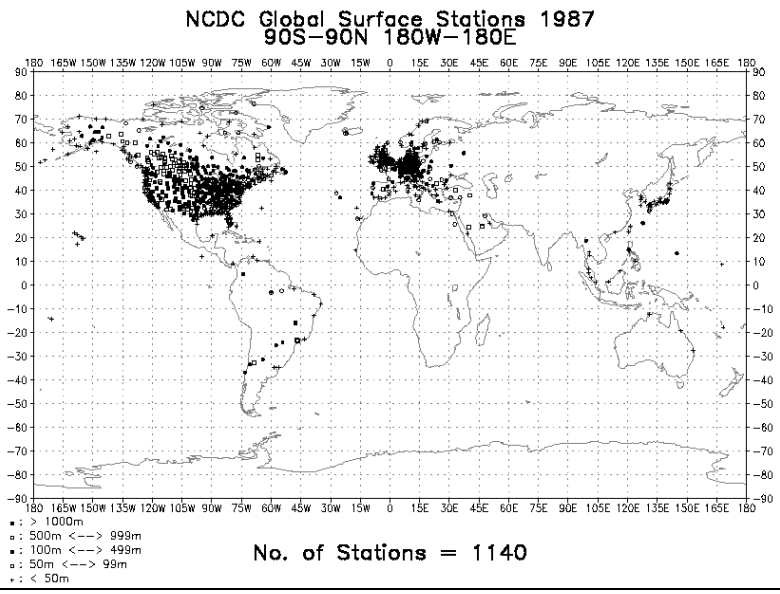

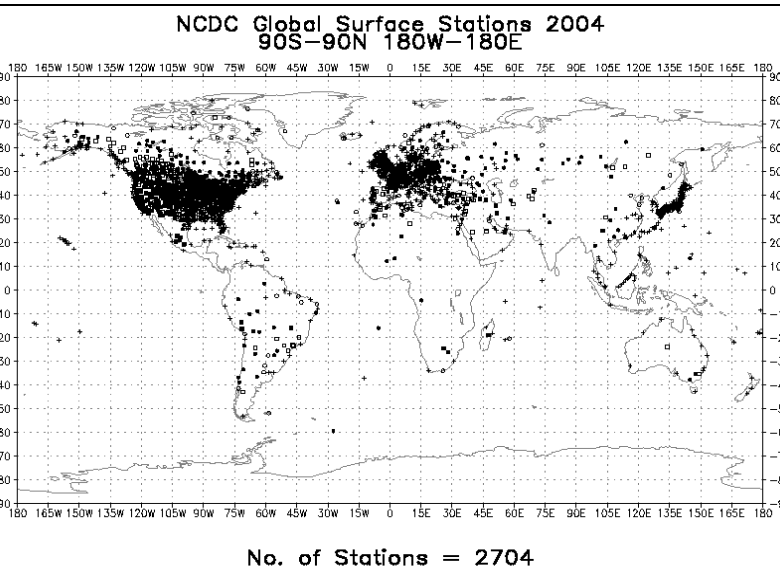

Figure V-A.1: Top (a) and bottom (b) figures show distribution of NCEI stations meeting 85% selection criteria for 1987 and 2004, respectively.

For the year 1987, 1139 stations passed our 85% selection criteria yielding 415,645 matching pairs on NCEI/GEOS-4 values; for 2004, 2697 stations passed yielding 987,451 matching pairs of NCEI/GEOS-4 temperature values. The color bar along the right side of the scatter plot provides a measure of the distribution of the NCEI/GEOS-4 temperature pairs. For example, in Figure V-A.2 each data point shown in dark blue represents a 1-degree cell with 1 to 765 matching temperature pairs, and all of the 1-degree cells shown in dark blue contain 15.15% of the total number of ground site points. Likewise, the darkest orange color represent 1-degree cells for which there are from 6120 to 6885 matching temperature pairs, and taken as a group all of the 1-degree cells represented by orange contain 10.61% of the total number of matching

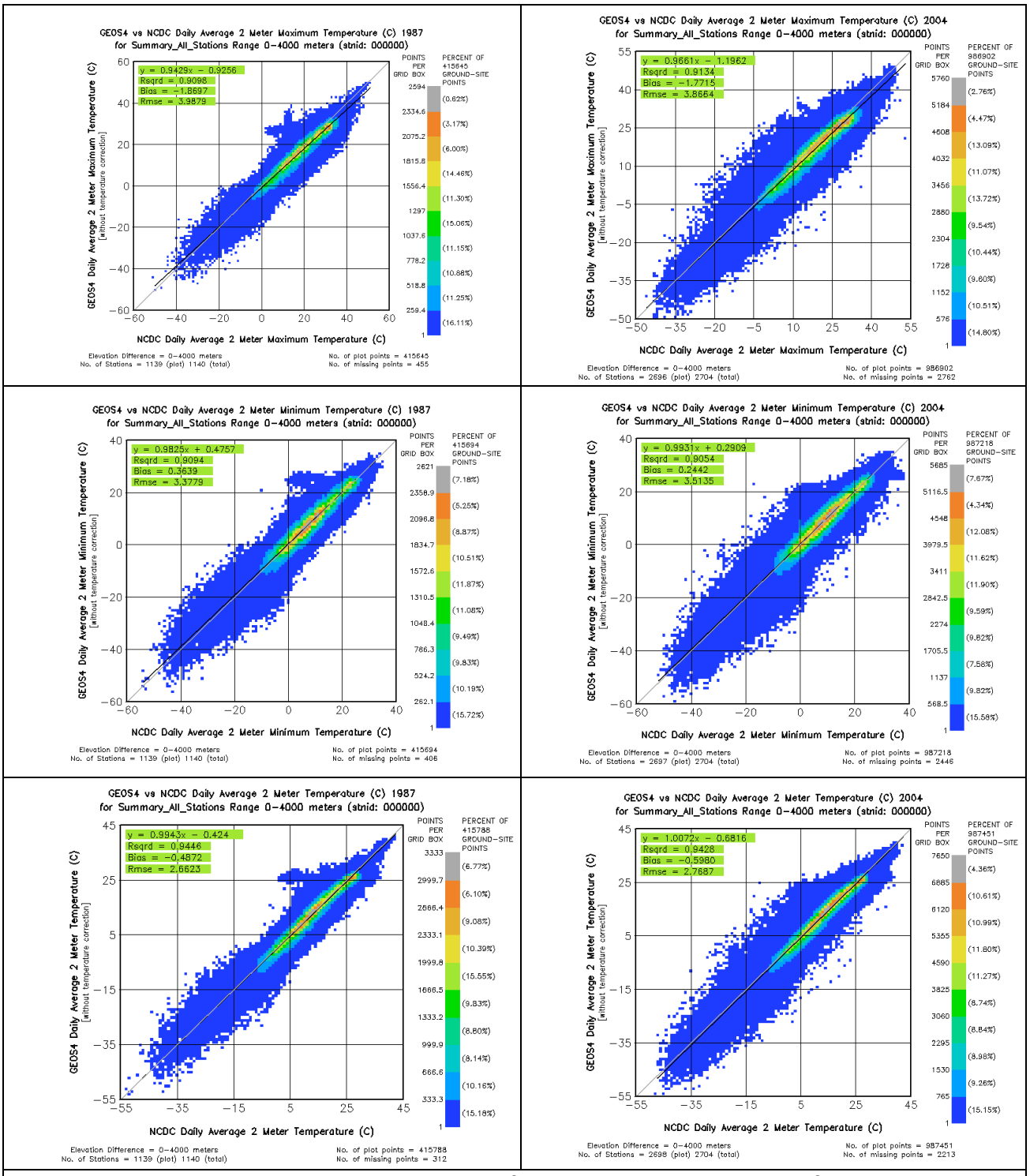

Figure V-A.2. Top (a), middle (b) and bottom (c) figures show the scatter plot of ground site observations versus GEOS-4 values of Tmax, Tmin, and Tave for the years 1987 and 2004. The color bar in each figure indicates the number and percentage of ground stations that are included within each color range.

ground site points. Thus, for the data shown in Figure V-A.2a, approximately 85% of matching temperature pairs (i.e. excluding the data represented by the dark blue color) is "tightly" grouped along the 1:1 correlation line.

In general, the scatter plots shown in Figure V-A.2, and indeed for all the years from 1983 through 2006, exhibit good agreements between the GEOS-4 data and ground observations. Notice however that for both the 1987 and 2004 data, on a global basis, the GEOS-4 Tmax values are cooler than the ground values (e.g. bias = -1.9 C in 1987 and -1.8 C in 2004); the GEOS-4 Tmin values are warmer (e.g. bias = 0.4 ^{o} C in 1987 and 0.2 ^{o} C in 2004); and that GEOS-4 Tave values are cooler (e.g. bias = -0.5 ^{o} C in 1987, and -0.6 ^{o} C in 2004. Similar trends in the respective yearly averaged biases between GEOS-4 and NCEI observations were noted for each year from 1983 – 2006 (see Table V-A.1 below). The ensemble average for the years 1983 – 2006 yields a GEOS-4 Tmax which is 1.82^{o} C cooler than observed at NCEI ground Sites, a Tmin about 0.27^{o} C warmer, and a Tave about 0.55^{o} C cooler. Similar trends are also observed for measurements from other meteorological networks. For example, using the US National Weather Service Cooperative Observer Program (COOP) observations, White, et al (2008) found the mean values of GEOS-4 Tmax, Tmin, and Tave to be respectively 2.4^{o} C cooler, Tmin 1.1^{o} C warmer, and 0.7 ^{o} C cooler that the COOP values.

Table V-A.1 Global year-by-year comparison of daily Tmax, Tmin, and Tave: NCEI GSOD values vs GEOS-4 temperatures

	Tmax					Tmin					Tave				
Year	Slope	Intercept (C)	R^2	RMSE (C)	Bias (C)	Slope	Intercept (C)	R^2	RMSE (C)	Bias (C)	Slope	Intercept (C)	R^2	RMSE (C)	Bias (C)
2006	0.97	-1.28	0.92	3.88	-1.72	1.00	0.09	0.90	3.59	0.11	1.02	-0.79	0.94	2.82	-0.59
2005	0.97	-1.40	0.92	4.00	-1.92	0.99	0.20	0.91	3.57	0.16	1.01	-0.81	0.95	2.81	-0.67
2004	0.97	-1.20	0.91	3.86	-1.78	0.99	0.28	0.91	3.50	0.24	1.01	-0.69	0.94	2.76	-0.60
2003	0.95	-0.91	0.91	3.96	-1.74	0.99	0.46	0.91	3.49	0.38	1.00	-0.47	0.94	2.82	-0.53
2002	0.94	-0.88	0.91	4.06	-1.94	0.98	0.47	0.90	3.55	0.30	0.98	-0.48	0.94	2.85	-0.66
2001	0.97	-1.69	0.92	4.00	-2.20	1.00	0.10	0.90	3.62	0.11	1.01	-0.97	0.95	2.78	-0.81
2000	0.97	-1.17	0.91	3.84	-1.67	1.00	0.25	0.91	3.50	0.27	1.01	-0.65	0.94	2.77	-0.52
1999	0.97	-1.25	0.91	3.80	-1.78	0.99	0.47	0.91	3.37	0.39	1.00	-0.60	0.95	2.63	-0.54
1998	0.98	-1.29	0.92	3.67	-1.71	0.99	0.11	0.91	3.27	0.07	1.01	-0.81	0.94	2.62	-0.68
1997	0.97	-1.20	0.92	3.64	-1.66	0.99	-0.01	0.91	3.30	-0.05	1.00	-0.72	0.95	2.67	-0.68
1996	0.95	-0.71	0.91	3.67	-1.56	0.98	0.27	0.91	3.31	0.15	0.99	-0.46	0.94	2.66	-0.55
1995	0.97	-1.44	0.92	3.93	-1.91	1.00	0.32	0.92	3.44	0.29	1.01	-0.69	0.95	2.69	-0.60
1994	0.98	-1.58	0.92	4.08	-1.93	1.00	-0.01	0.91	3.55	-0.04	1.01	-0.82	0.95	2.85	-0.71
1993	0.96	-1.22	0.92	3.93	-1.80	0.99	0.22	0.92	3.40	0.16	1.00	-0.51	0.95	2.68	-0.52
1992	0.95	-0.92	0.91	3.90	-1.70	0.98	0.43	0.90	3.46	0.33	1.00	-0.43	0.94	2.67	-0.43
1991	0.95	-1.05	0.91	4.14	-1.89	0.99	0.35	0.91	3.45	0.27	1.00	-0.45	0.94	2.80	-0.49
1990	0.95	-1.12	0.90	4.18	-1.94	0.99	0.40	0.91	3.49	0.35	1.00	-0.44	0.94	2.79	-0.49
1989	0.96	-1.18	0.91	4.15	-1.91	0.99	0.48	0.92	3.50	0.42	0.99	-0.40	0.95	2.79	-0.46
1988	0.95	-1.11	0.91	4.03	-1.90	0.99	0.55	0.91	3.38	0.47	1.00	-0.38	0.95	2.63	-0.42
1987	0.94	-0.93	0.91	3.99	-1.87	0.98	0.48	0.91	3.38	0.36	0.99	-0.42	0.94	2.66	-0.49
1986	0.95	-1.02	0.91	4.05	-1.88	0.98	0.52	0.91	3.37	0.39	0.99	-0.35	0.94	2.70	-0.45
1985	0.96	-1.11	0.92	4.03	-1.84	0.99	0.38	0.92	3.58	0.32	0.99	-0.44	0.95	2.83	-0.49
1984	0.96	-1.07	0.91	4.00	-1.79	1.00	0.44	0.91	3.46	0.41	1.00	-0.45	0.94	2.79	-0.47
1983	0.96	-1.19	0.91	4.02	-1.78	0.99	0.41	0.91	3.44	0.34	1.00	-0.49	0.94	2.82	-0.52
Average	0.96	-1.16	0.91	3.95	-1.82	0.99	0.32	0.91	3.46	0.26	1.00	-0.57	0.94	2.75	-0.56
STDEV	0.01	0.22	0.01	0.15	0.13	0.01	0.17	0.01	0.10	0.14	0.01	0.17	0.00	0.08	0.10

The average of the least square fit along with the average RMSE and Bias values given in Table V-A.1 are taken as representative of the agreement expected between GEOS-4 temperatures and ground site measurements

Further analysis, described in Appendix A, shows that one factor contributing to the temperature biases between the assimilation model estimates and ground site observations is the difference in the elevation of the reanalysis grid cell and the ground site. Appendix A describes a downscaling methodology based upon a statistical calibration of the assimilation temperatures relative to ground site observations. The resulting downscaling parameters (i.e. lapse rate and

offset values) can be regional and/or seasonally focused and result in estimates of local temperatures with reduced biases relative to ground site observations.

Application of the downscaling procedure described in Appendix A is not currently implemented in the Agroclimatological archive, and is describe herein for users that might need more accurate estimates of local temperatures.

(Return to Content)

V.Cii. Assessment of GEOS-5 Temperatures*:* An initial assessment of the GEOS-5 temperatures follows the methodology described above for the GEOS-4 temperatures. Results from the assessment, which included 4.172 globally distributed ground stations reporting observations in the NCEI GSOD files for the year 2009, are given in Table VII-A.3.

Table V-A.3. Summary of statistics for a global comparison of the uncorrected GEOS-5 daily temperatures to ground observations reported by 4172 stations in the NCEI GSOD files during 2009

Parameter	Bias	RMSE	Slope	Intercept	R^2	Daily Values
Tave	-0.98	3.15	0.96	-0.74	0.92	1,214,462
Tmax	-1.07	3.62	0.97	-0.58	0.93	1,518,601
Tmin	0.84	3.68	0.97	1.05	0.91	1,519,039

(Return to Content)

V. B. Relative Humidity: The relative humidity (RH) values in the POWER archives are calculated from pressure (P_a in kPa), dry bulb temperature (T_a in $^{\circ}$C), and mixing ratio (e.g. specific humidity, q in kg/kg), parameters that are available in the NASA's MERRA assimilation model. The following is a summary of the expressions used to calculate RH. The units are indicated in square brackets.

From Iribarne and Godson (1981) a fundamental definition of the Relative Humidity (Eq. 83, pg 75):

(V.B.1) $$RH = (e_a/e_{sat}) \times 100\%$$

where

e_a = the water vapor pressure and

e_{sat} the saturation water vapor pressure at the ambient temperature Ta.

The 100% has been added to cast RH in terms of percent.

Since water vapor and dry air (a mixture of inert gases) can be treated as ideal gases, it can be shown that (Iribarne and Godson, pg 74, Eq. 76; Note that the symbol, r, use in Eq. 76 for the

mixing ratio has been replaced by "w" and the factor of "10" has been added to convert the units to hPa.)

(V.B.2) $e_a = (10 \times P_a \times w)/(\varepsilon + w)$ [hPa]

where w is the mixing ratio define as the ratio of mass of water to dry air and

(V.B.3) $$\epsilon = \frac{R'}{R_v} = \frac{287.05}{461.5} \simeq 0.622$$

where R' and R_v are the dry and water vapor gas constants respectively (note that there is no exact consensus for the gas constants past 3 significant digits, therefore the value of the ratio is kept to 3 significant digits). The mixing ratio is related to specific humidity by the relation (Jupp 2003, pg.37):

(V.B.4) $w = q / (1-q)$ [kg/kg]

Combining (VII.B.2) and (VII.B.4) leads to the following expression for e in terms of q:

(V.B.5) $e_a = q \times 10 \times P_a/[\varepsilon + q \times (1- \varepsilon)]$ [hPa]

An eighth-order polynomial fit (Flatau, et. al. 1992) to measurements of vapor pressure over ice and over water provides an expression to calculate the saturated water vapor pressure over ice and over water. The eight-order fit for e_{satw} is given by

(V.B.6) $e_{wsat} = A_{1w} + A_{2w} \times (T_a) + \ldots + A_{(n-1)w} \times (T_a)^n$

and

(V.B.7) $e_{isat} = A_{1i} + A_{2i} \times (T_a) + \ldots + A_{(n-1)i} \times (T_a)^n$,

Where

e_{wsat} = saturated vapor pressure over water in [hPa = mb]

e_{isat} = saturated vapor pressure over ice [hPa=mb]

T_a is the ambient dry bulb temperature in ^oC.

Table V.B.1 gives the coefficients for e_{sat} over water and over ice and the temperature range over which the coefficient are applicable.

Table V.B.1. Coefficients of the eight-order polynomial fit (Taken from Flatau, et. al. 1992 Table 4.) to measurements of saturated vapor pressure measurements,	
Coefficients for e_{sat} over water valid over the temperature range -85 ^{o}C to +70 ^{o}C	Coefficients for e_{sat} over ice valid over the temperature range -90 ^{o}C to 0 ^{o}C
A1w = 6.11583699	A1i = 6.09868993
A2w = 0.444606896	A2i = 0.499320233
A3w = 0.143177157E-1	A3i = 0.184672631E-1
A4w = 0.264224321E-3	A4i = 0.402737184E-3
A5w = 0.299291081E-5	A5i = 0.565392987E-5
A6w = 0.203154182E-7	A6i = 0.521693933E-7
A7w = 0.702620698E-10	A7i = 0.307839583E-9
A8w = 0.379534310E-13	A8i = 0.105758160E-11
A9w = -0.321582393E-15	A9i = 0.161444444E-14

Note that only the relative humidity over water is calculated and provided in the POWER/Sustainable Buildings Archive consistent with the values reported by the National Weather Service..

GEOS-4 Relative Humidity: Table VII-B.2 Summarizes the comparison statistics for the relative humidity based upon GEOS-4 q, P, T values vs. ground observations reported in the 2007 National Center for Environmental Information (NCEI – formally National Climatic Data Center) GSOD files.

(**Note that for the comparison statistics in Tables VII-B.2 and –B.3 the RH was calculated using a different approximation for calculating RH, however the percentage differences in the RH values was typically less the 10%.)**

Table V-B.2. Summary of statistics for a global comparison of the daily mean relative humidity based upon GEOS-4 q, P, T values to ground observations reported in the NCEI GSOD files during 2007.

Bias	RMSE	Slope	Intercept	R^2	Daily Values
-1.89	12.67	0.76	1.62	0.55	1,214,462

GEOS-5 Relative Humidity: Table VII-B.3 Summarizes the comparison statistics for the relative humidity values based upon GEOS-5 q, P, and T vs. ground observations reported in the 2009 NCEI GSOD files.

Table V-B.3. Summary of statistics for a global comparison of the daily mean relative humidity based upon GEOS-5 q, P, T values to ground observations reported in the NCEI GSOD files during 2009.

Bias	RMSE	Slope	Intercept	R^2	Daily Values
-0.95	11.79	0.81	0.24	0.61	1,428,047

(Return to Content)

V. C. Dew/Frost Point Temperatures: The daily dew and frost point temperatures, DFpt, are calculated from the relative humidity, RH, and temperature , T_a. The following is a summary of the methodology used to calculate DFpt.

(1) $RH_1 = 1.0 - RH/100$

Where RH is calculated, as described in Section V.B, using the specific humidity, pressure, and temperature taken from the assimilation model.

The DFpt is calculated using the expression (Encyclopedia Edited by Dennis R. Heldman)

(2) $DFpt = T_a - \{(14.55 + .114 \times T_a) \times RH_1 + [(2.5 + 0.007 \times T_a) \times RH_1]^3 + (15.9 + 0.117 \times T_a) \times (RH_1)^{14}\}$

The following tables give the statistics associated with comparing the dew/frost point temperatures based upon GEOS-4 RH and T_a values (Table VII-C.1) and GEOS-5 RH and T_a values (Table VII-C.2).

(**Note that for the comparison statistics in Tables VII-C.1 and –C.2 the RH was calculated using a different approximation for calculating RH, however the differences in the dew point temperatures ranging from approximately -50C to 40C was less than 1C.)**

Table V-C.1. Summary of statistics for a global comparison of the GEOS-4 daily mean dew point to ground observations reported by 3410 station in the NCEI GSOD files during 2007.

Bias	RMSE	Slope	Intercept	R^2	Daily Values
-0.98	3.15	0.96	-0.74	0.92	1,214,462

Table V-C.2. Summary of statistics for a global comparison of the GEOS-5 daily mean dew point to ground observations reported by 4172 stations the NCEI GSOD files during 2009.

Bias	RMSE	Slope	Intercept	R^2	Daily Values
-0.43	3.03	0.95	-0.16	0.92	1,428,047

(Return to Content)

D. Precipitation: The precipitation data in POWER/Agroclimatology archive has been obtained from version 2.1 Global Precipitation Climate Project (GPCP – 1DD) Satellite-Gauge Product http://precip.gsfc.nasa.gov). Version 2.1, is a global 1°x1° daily accumulation based upon combination of observations from multiple platforms described at http://precip.gsfc.nasa.gov/gpcp_v2.1_comb_new.html and synopsized below as:

Version 2.1 Global Precipitation Climate Project Satellite-Gauge Product

1. Special Sensor/Microwave Imager (SSM/I; 0.5°x0.5° by orbit, GPROF algorithm) provides fractional occurrence of precipitation, and
2. GPCP Version 2 Satellite-Gauge (SG) combination (2.5°x2.5° monthly) data provides monthly accumulation of precipitation as a "scaling constraint" that is applied to the algorithms use to estimate precipitation values from :
   a. geosynchronous-orbit IR (geo-IR) T_b histograms (1°x1° grid in the band 40°N-40°S, 3-hourly),
   b. low-orbit IR (leo-IR) GOES Precipitation Index (GPI; same time/space grid as geo-IR),
   c. TIROS Operational Vertical Sounder (TOVS; 1°x1° on daily nodes, Susskind algorithm), and
   d. Atmospheric Infrared Sounder (AIRS; 1°x1° on daily nodes, Susskind algorithm).

In general, precipitation often tends to be a rather localized and short duration event. Consequently, accurately capturing the amount of precipitation, even in terms of mean daily amounts, from satellite observation is challenging. The GPCP -1DD data were used as the base precipitation source since it is derived from inputs from multiple platforms and therefore was deemed to have a better chance of capturing daily rainfall events.

It is noted that the Tropical Rainfall Measurement Mission (TRMM - http://trmm.gsfc.nasa.gov/) is another potential source for precipitation data, however it's polar orbit combined with a ¼ - degree resolution limits the daily coverage that can be provided for a given location. Moreover the global coverage afforded by TRMM is nominally from 40N to 40S latitude. Currently the TRMM data is not included as part of the POWER/Agroclimatology precipitation data product.

Numerous validation studies of the GPCP data products have been published (Adler, et. al. 2003; McPhee and Margulis , 2005; references cited in these publications), however, analysis/validation of the GPCP 1-degree daily products have, in general, been based upon methodologies that temporally and/or spatially average the precipitation data. In the remainder of this section, validations based upon comparisons of the daily 1-degree precipitation values obtained from the POWER/Agroclimatology archive to corresponding ground sites observation within the same 1-degree cell are discussed.

We first show results comparing GPCP – 1DD data and ground site observations from the single 1-degree cell shown in Figure V-E.1. Figure V-E.1 shows the location of three ground sites in Louisiana all within a 1-degree grid cell bounded by on the North and South by 32N and 31S latitudes respectively and on the East and West by 92W and 93W longitudes respectively. Daily mean precipitation data measured at these three sites over a 9-year period beginning in 1997 were compared to daily mean values available from the POWER/Agroclimatology archive. Figures V-E.2a, b, and c show scatter plots of the POWER values versus ground site measurements for accumulation over 1-day, 5-day and for a 30-day accumulation.

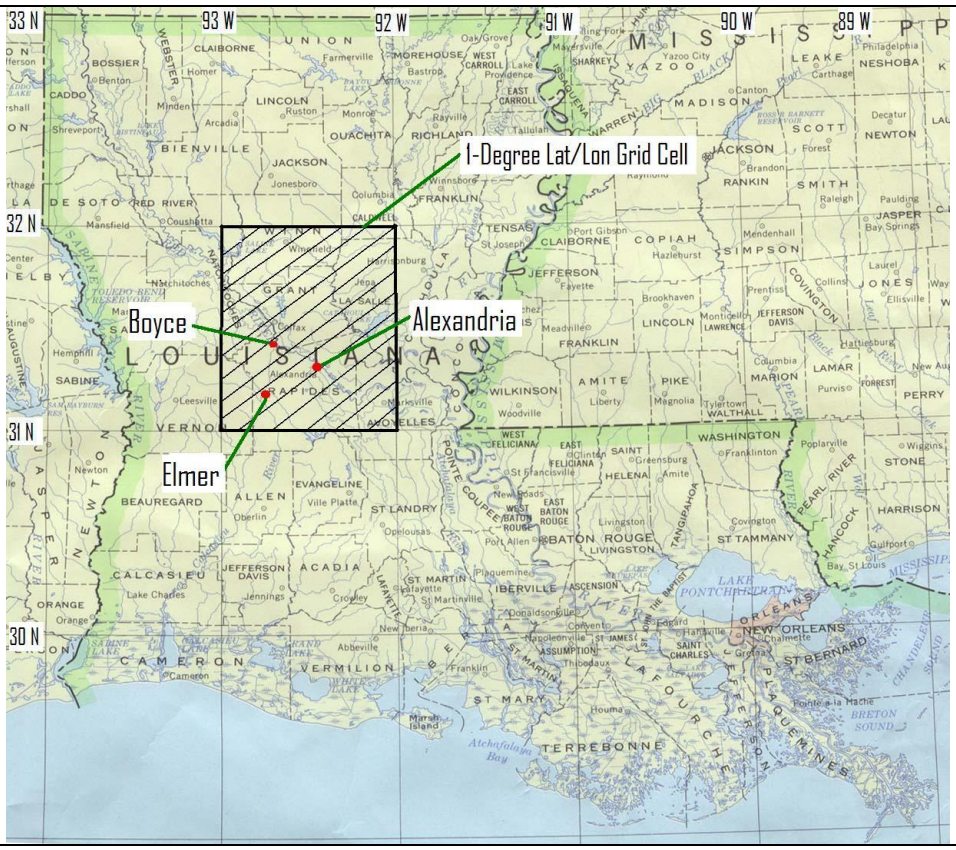

Figure V-E.1 Location of the three ground sites in Louisiana used in the precipitation comparative study and the 1-degree grid cell over which the GPCP precipitation is averaged.

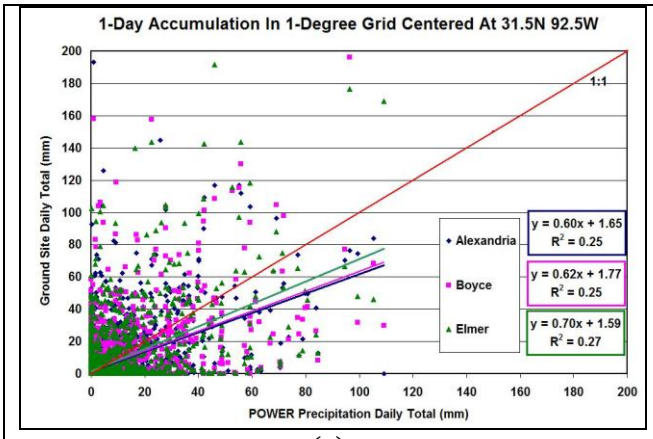

(a)

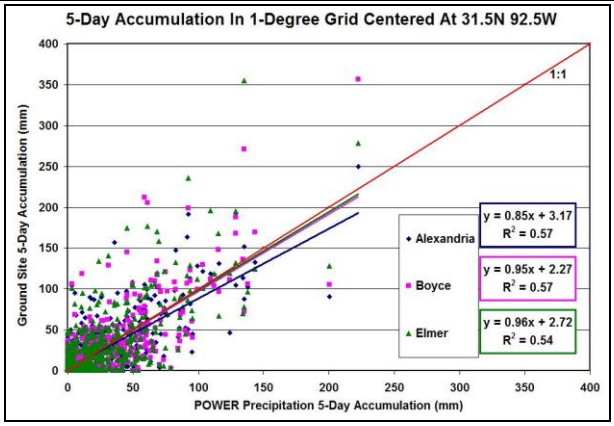

(b)

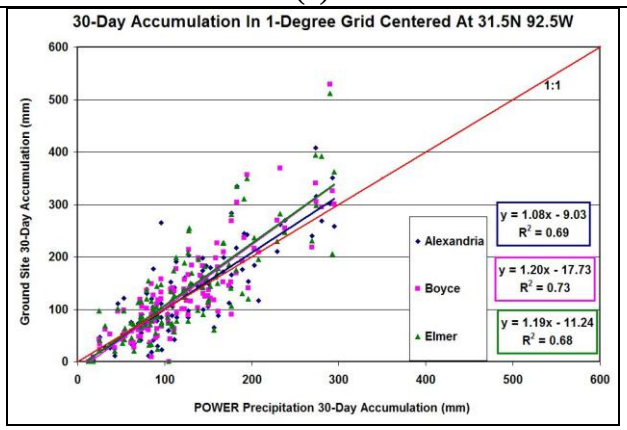

(c)

Figures V-E.2. Scatter plots of ground site measurements and GPCP data for the accumulation over (a) 1-day, (b) 5-day, and (c) 30-day accumulation periods computed from precipitation data covering the 1997 – 2005 years.

The results of a cell-by-cell comparison of the daily values from POWER/Agroclimatology and ground observation within the Continental United States (CONUS) is summarized in Figures V-E.3 and -4. The ground site observations were reported in the NCEI GSOD files for the year 2004, and the GPCP values are from the POWER/Agroclimatology archive. Figure V-E.3 shows the distribution of the NCEI sites for 2004, and Figure V-E.4 shows the cell-by-cell scatter plot of the ground and POWER/Agroclimatology values for (a) a 30-day accumulation and (b) 1-day accumulation.

The results from the single cell and the CONUS cell-by-cell comparison echo the results, implicit in the methodology used by McPhee and Margulis (2005) where only spatial (regional) and temporally (seasonal) averaged comparisons were reported and by Bolvin, et. al. (2009). Namely, the agreement between the GPCP 1-DD data products and ground observations improves with temporal (and spatial) averaging.

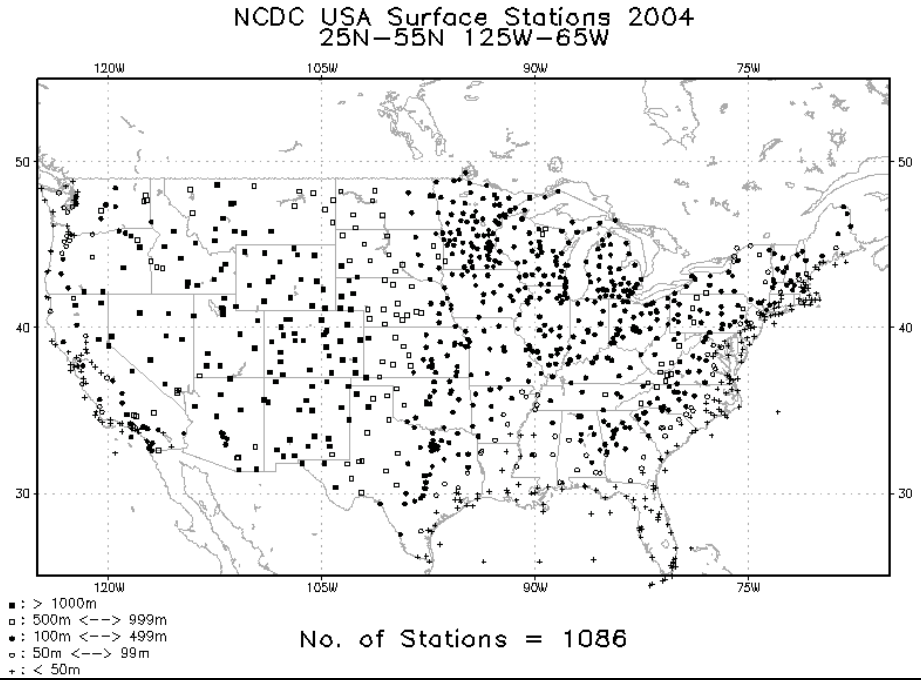

Figure V-E.3 Location of the NCEI ground sites used for comparison with estimates from the GPCP 1-DD archive.

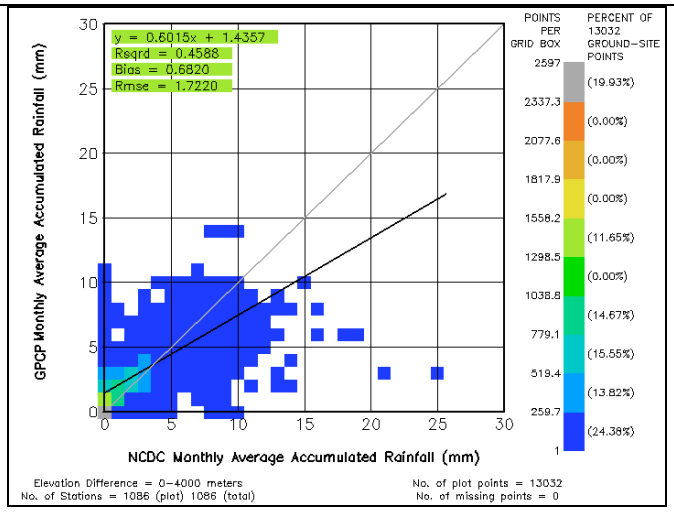

(a) Monthly averaged.

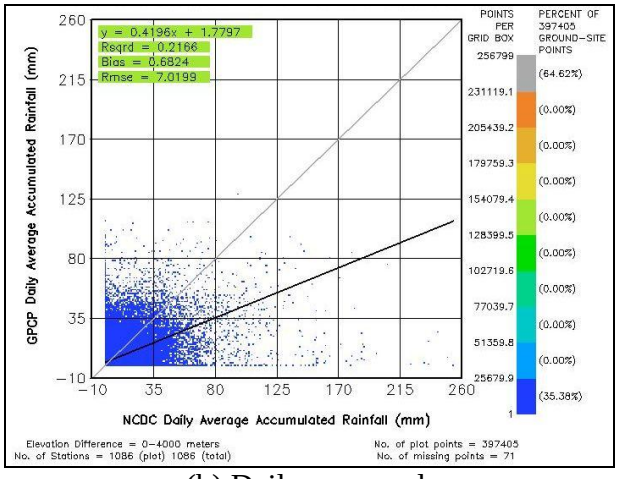

(b) Daily averaged.

Figures V-E.4. Scatter plots of cell-by-cell ground site measurements and GPCP data for the accumulation over (a) 1-month and (b) 1-day to ground site observation for the year 2004.

Table V-E.1.Summary of comparison statistics associated with the scatter plots shown in Figure V-E.4.		
Parameter	Daily Data	Monthly Data
Slope:	0.4196	0.6015
Intercept:	1.7797 mm	1.4357 mm
Rsqrd:	0.2166	0.4588
Bias:	0.6824 mm	0.682 mm
Absolute Bias:	2.6016 mm	1.14017 mm
Rmse:	7.0199 mm	1.722 mm
GPCP Mean:	2.57308 mm	2.5735 mm
GPCP Std Dev:	6.3839 mm	1.835 mm
NCEI Mean:	1.89072 mm	1.8915 mm
NCEI Std Dev:	7.0807 mm	2.0665 mm

(Return to Content)

V-E. Daily Mean Wind Speed: For the time period January 1, 1983 – December 31, 2007 the daily means winds in the POWER/Agroclimatology archive are from the GEOS-4 assimilation model. For the time period January 1, 2008 to within several days of current time the daily means winds are from the GEOS-5 assimilation model. The model winds are at 10m elevation above the Earth's surface. Testing of these winds was performed through comparison with wind measurements reported in the NCEI GSOD files.

GEOS-4 Winds: Comparison of ground site observation reported in the NCEI GSOD files with the 10m GEOS-4 winds for various time periods and regions have typically resulted in the GEOS-4 values being about ½ the ground observations. Table V-E.1 gives the yearly averaged bias, RMSE, slope, intercept, and R^2 for a global comparisons of 2007 wind data. The last column in this table gives the total number of daily values in the comparison.

Table V-E.1 Summary of statistics for comparison of GEOS-4 10m daily winds to ground observations during 2007.					
Bias	**RMSE**	**Slope**	**Intercept**	**R^2**	**Daily Values**
0.011	1.76	0.55	1.62	0.42	1,224,453

GEOS-5 Winds: Table V-E.2 gives the bias, RMSE, slope, intercept, R^2, and total number of daily values for a global comparisons of the 2009 GEOS-5 daily mean winds with values reported in the NCEI GSOD files.

Table V-E.2 Summary of statistics for comparison of GEOS-5 10m daily winds to ground observations during 2009.					
Bias	**RMSE**	**Slope**	**Intercept**	**R^2**	**Daily Values**
0.38	1.83	0.65	1.62	0.46	956,263

(Return to Content)

IX. References

Adler, R.F., G.J. Huffman, A. Chang, R. Ferraro, P. Xie, J. Janowiak, B. Rudolf, U. Schneider, S. Curtis, D. Bolvin, A. Gruber, J. Susskind, P. Arkin, E. Nelkin 2003: The Version 2 Global Precipitation Climatology Project (GPCP) Monthly Precipitation Analysis (1979-Present). *J. Hydrometeor.*, **4**, 1147-1167.

Bai, J., X. Chen, A. Dobermann, H. Yang, K.G. Cassman, and F. Zhang. 2010. Evaluation of NASA satellite- and model-derived weather data for simulation of maize yield potential in China. Agron. J. 102:9–16. doi:10.2134/agronj2009.0085

Blandford, Troy R., Karen S. Blandford, Bruan J. Harshburger, Brandon C. Moore, and Von P. Walden. Seasonal and Synoptic Variations in near-Surface Air Temperature Lapse Rates in a Mountainous Basin. J. Applied Meteorology and Climatology. 2008, Vol. 47, 249 – 261.

Bloom, S., A. da Silva, D. Dee, M. Bosilovich, J.-D. Chern, S. Pawson, S. Schubert, M. Sienkiewicz, I. Stajner, W.-W. Tan, M.-L. Wu, Documentation and Validation of the Goddard Earth Observing System (GEOS) Data Assimilation System - Version 4, Technical Report Series on Global Modeling and Data Assimilation, NASA/TM—2005–104606, Vol. 26, 2005

Bolvin, David T., Robert F. Adler, George J. Huffman, Eric J. Nelkin, Jani P. Poutiainen, 2009: Comparison of GPCP Monthly and Daily Precipitation Estimates with High-Latitude Gauge Observations. *J. Appl. Meteor. Climatol.*, **48**, 1843–1857. doi: 10.1175/2009JAMC2147.1

Braun, J. E. and J. C. Mitchell, 1983: Solar Geometry for Fixed and Tracking Surfaces. Solar Energy, Vol. 31, No. 5, pp. 439-444.

Briggs, Robert S., R. G. Lucas, Z. T. Taylor, 2003: Climate Classification for Building Energy Codes and Standards. Technical Paper, Pacific NW National Laboratory, March 26, 2002. Continue to use original climate zone definitions.

Collares-Pereira, M. and A. Rabl, 1979: The Average Distribution of Solar Radiation-Correlations Between Diffuse and Hemispherical and Between Daily and Hourly Insolation Values. Solar Energy, Vol. 22, No. 1, pp. 155-164.

Dorman, J. L. and P. J. Sellers, 1989: A Global Climatology of Albedo, Roughness Length and Stomatal Resistance for Atmospheric General Circulation Models as Represented by the Simple Biosphere Model (SiB). Journal of Atmospheric Science, Vol. 28, pp. 833-855.

Encyclopedia of Agricultural, Food, and Biological Engineering edited by Dennis R. Heldman Page 189

Erbs, D. G., S. A. Klein, and J. A. Duffie, 1982: Estimation of the Diffuse Radiation Fraction for Hourly, Daily and Monthly average Global Radiation. Solar Energy, Vol. 28, No. 4, pp. 293-302.

Gipe, Paul, 1999: Wind Energy Basics, Chelsea Green Publishing, 122 pp.

Gupta, S. K., D. P. Kratz, P. W. Stackhouse, Jr., and A. C. Wilber, 2001: The Langley Parameterized Shortwave Algorithm (LPSA) for Surface Radiation Budget Studies. NASA/TP-2001-211272, 31 pp. Available on-line at: http://ntrs.nasa.gov/search.jsp

Harlow, R. C., E. J. Burke, R. L. Scott, W. J. Shuttleworth, C. M. Brown, and J. R. Petti. Derivation of temperature lapse rates in semi-arid south-eastern Arizona, (2004) Hydrol. and Earth Systems Sci, 8(6) 1179-1185.

Klein, S.A., 1977: Calculation of monthly average insolation on tilted surfaces. Solar Energy, Vol. 19, pp. 325-329.

Liu, B. Y. H. and R. C. Jordan, 1960: The Interrelationship and Characteristic Distribution of Direct, Diffuse, and Total Solar Radiation. Solar Energy, Vol. 4, No. 3, pp. 1-19.

Lookingbill, Todd R. and Dean L. Urban, Spatial estimation of air temperature differences for landscape-scale studies in mountain environments, (2003) Agri. and Forst. Meteor, 114(3-4) 141-151.

McPhee, James, Steven A. Margulis, 2005: Validation and Error Characterization of the GPCP-1DD Precipitation Product over the Contiguous United States. *J. Hydrometeor*, **6**, 441–459. doi: 10.1175/JHM429.1

Ohmura, Atsumu, Ellsworth G. Dutton, Bruce Forgan Claus Fröhlich Hans Gilgen, Herman Hegner, Alain Heimo, Gert König-Langlo, Bruce McArthur, Guido Mueller, Rolf Philipona, Rachel Pinker, Charlie H. Whitlock, Klaus Dehne, and Martin Wild, 1998: Baseline Surface

Pinker, R., and I. Laszlo, 1992: Modeling Surface Solar Irradiance for Satellite Applications on a Global Scale. *J. Appl. Meteor.,* 31, 194–211.

Radiation Network (BSRN/WCRP): New Precision Radiometry for Climate Research, Bull. Of American Meteor. Soc., **79**, 10, p 2115-2136.

RETScreen: Clean Energy Project Analysis: RETScreen® Engineering & Cases Textbook, Third Edition, Minister of Natural Resources Canada, September 2005. (http://www.retscreen.net/ang/12.php, Engineering e-Textbook, Version 4, RETScreen

Photovoltaic Project Analysis Chapter, pp. PV.15-PV.21, ISBN: 0-662-35672-1, Catalogue no.: M39-99/2003E-PDF).

Rossow, W.B., and R.A. Schiffer, 1999: Advances in understanding clouds from ISCCP. *Bull. Amer. Meteorol. Soc.*, **80**, 2261-2288, doi:10.1175/1520-0477(1999)080<2261:AIUCFI>2.0.CO;2.

Schwartz, Marc, 1999: Wind Energy Resource Estimation and Mapping at the National Renewable Energy Laboratory. NREL Conf. Pub. NREL/CP-500-26245.

Smith, G.L., R. N. Green, E. Raschke, L. M. Avis, J. T. Suttles, B. A. Wielicki, and R. Davies, 1986: Inversion methods for satellite studies of the Earth's radiation budget: Development of algorithms for the ERBE mission. Rev. Geophys., 24, 407-421.

Surface Weather Observations and Reports, Federal Meteorological Handbook No. 1, FCM-H1-2005, Washington, D.C., 2005

Rasch, P. J., N. M. Mahowald, and B. E. Eaton (1997), Representations of transport, convection, and the hydrologic cycle in chemical transport models: Implications for the modeling of short-lived and soluble species, J. Geophys. Res., 102(D23), 28, 127-128, 138.

Takacs, L. L., A. Molod, and T. Wang, 1994: Volume 1: Documentation of the Goddard Earth Observing System (GEOS) general circulation model - version 1, NASA Technical Memorandum 104606, Vol. 1, 100 pp.

White, Jeffrey W. , Gerrit Hoogenboom, aul W. Stackhouse Jr., and James M. Hoell, Evaluation of NASA satellite- and assimilation model-derived long-term daily temperature data over the continental US, Agric. Forest Meteorol. (2008), doi:10.1016/j.agrformet.2008.05.017

White, Jeffrey W. , Gerrit Hoogenboom, Paul W. Wilkens, Paul W. Stackhouse Jr., and James M. Hoell, Evaluation of Satellite-Based, Modeled-Derived Daily Solar Radiation Data for the Continental United States**.** Agron. J. 103:1242-1251(2011)

(Return to Content)

Appendix A: **Downscaling Assimilation Modeled Temperatures**

In section V temperature estimates from the GEOS-4 assimilation model were found to exhibit a globally and yearly (1983 – 2006) averaged bias for Tmax of -1.82° C , for Tmin about +0.27°, for Tave about - 0.55° C relative to ground site observations. In this Appendix factors contributions to these biases are noted with the main focus being the description of a methodology that can reduce the biases for local ground site.

The spatial resolution of the GEOS-4 assimilation model's output is initially on a global 1^o by 1.25^o grid and then re-gridded to a spatial 1^o by 1^o grid to be spatially compatible with the solar insolation values available through the POWER archive. The elevation of original and re-gridded cell represents the average elevation of the earth's surface enclosed by the dimensions of the grid cell. Figure A.1 illustrates the spatial features associated with a reanalysis cell and a local ground site. In mountainous regions, in particular, the elevation of the grid cell can be substantially different from that of the underlying ground site.

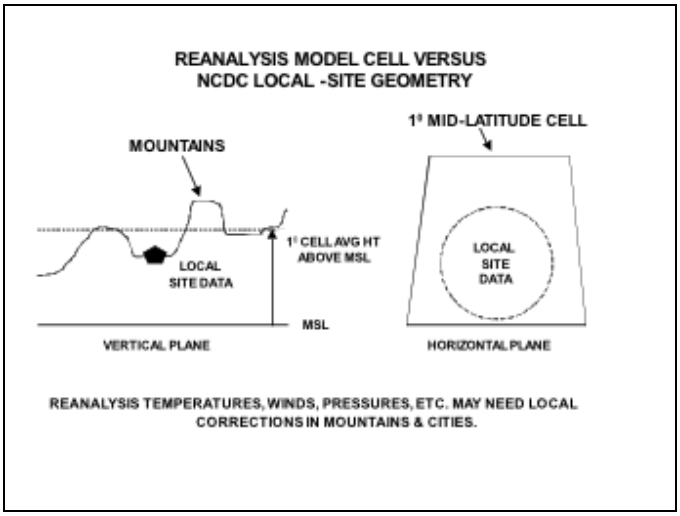

Figure A.1***:*** *Relative height and horizontal features associated with a nominal 1-degree cell and a local ground site in the mountains.*

The inverses dependence of the air temperature on elevation is well known and suggests that the elevation differences between the re-analysis grid cell and the actual ground site may be a factor contribution to the biases between the modeled and observed temperatures. In figure A-2, the yearly averaged differences between ground site measurements and reanalysis modeled values (i.e. bias) are plotted against the difference in the elevation of the ground site and the reanalysis grid for the ensemble of years 1983 – 2006. The stations have been grouped into 50m elevation difference bins (e.g. 0 to 50m; >50m to 100m; >100m to 150m; etc.) and plotted against the mean yearly bias for the respective elevation bin. The solid line is the linear least squares fit to the scatter plot and the parameters for the fit are given in the upper right hand portion of each plot. Table A-1 gives the parameters associated with linear regression fits to similar scatter plots for individual years and is included here to illustrate the year-to-year consistency in these

parameters. The linear dependence of the bias between the GEOS-4 and NCEI temperature values on the elevation difference between the GEOS-4 cell and ground elevation is clearly evident in Figure A-2 and Table A-1. The mean of the slope, intercept, and R^2 for the individual years is given in the row labeled "Average". The bottom row of Table A-1 lists the fit parameters of Figure A-2.

As already noted, the inverses dependence of the air temperature on elevation is well known with -6.5^{o}C/km typically accepted as a nominal global environmentally averaged lapse rate value (Barry and Chorely 1987). Moreover, numerous studies have been published (Blandford et al., 2008; Lookingbill et al., 2003; Harlow et al., 2004) that highlight the need to use seasonal and regionally dependent lapse rates for the daily Tmin and Tmax values to adjustment ground site observations to un-sampled sites at different elevations. In the remaining sections an approach to statistically calibrate the assimilation model and downscale the reanalysis temperatures to a specific site within the reanalysis grid box is described.

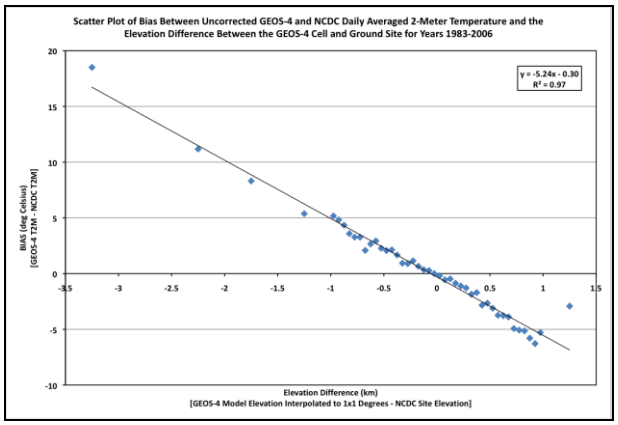

(a)

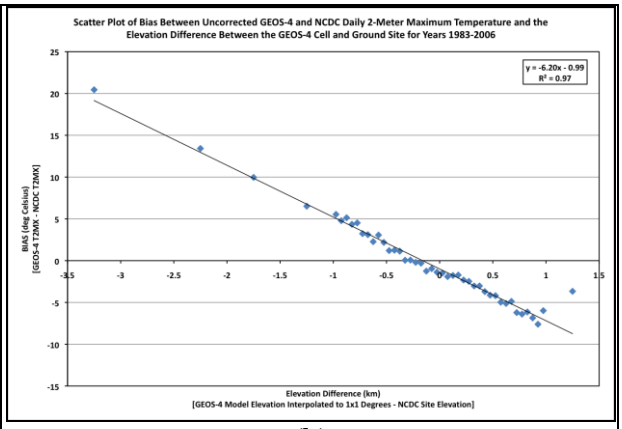

(b)

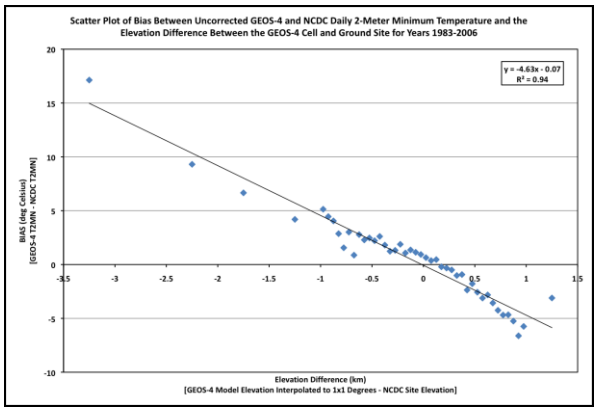

(c)

Figure A-2. Scatter plots showing the dependence of the bias between the GEOS-4 Tave (a), Tmin (b), and Tmax (c) temperatures and values from the NCEI archive on the elevation difference between the GEOS-4 cell and the ground station elevation for the years 1983 -2006. The elevation difference between stations are grouped into elevation difference bins (e.g. 0 to 50m; >50m to 100m; >100m to 150m; etc.) and plotted against the mean bias for the respective elevation bin.

Table A.1. Linear regression parameters associated with scatter plots of yearly mean bias between NCDC and GEOS-4 daily tenperatures and the elevation difference between the NCDC ground station and the GEOS-4 1-degree grid cell. Each row gives the regression parameters by year. For comparison, the bottom row gives the regression parameters from Figure A-2.

Year	Tmax			Tmin			Tave		
	Slope (c/km)	Intercept (C)	R^2	Slope (c/km)	Intercept (C)	R^2	Slope (c/km)	Intercept (C)	R^2
1983	-5.56	-0.85	0.85	-3.9	0.37	0.87	-4.71	0.03	0.92
1984	-5.82	-0.71	0.87	-4.18	0.43	0.89	-4.98	0.1	0.93
1985	-4.96	-1.01	0.85	-4.11	0.3	0.84	-4.71	-0.05	0.94
1986	-5.64	-0.86	0.86	-4.11	0.31	0.84	-4.97	0.03	0.92
1987	-5.01	-1.17	0.82	-4.76	0.55	0.91	-4.84	-0.06	0.94
1988	-5.55	-0.91	0.83	-4.38	0.4	0.84	-4.95	0.04	0.9
1989	-5.37	-1.11	0.87	-3.82	0.15	0.81	-4.5	-0.23	0.9
1990	-6.7	-0.61	0.94	-4.85	0.3	0.9	-5.64	0.13	0.95
1991	-6.66	-0.41	0.93	-4.94	0.5	0.92	-5.73	0.32	0.96
1992	-6.29	-0.34	0.89	-5.09	0.75	0.91	-5.49	0.33	0.94
1993	-6.14	-0.35	0.89	-5.02	0.75	0.89	-5.5	0.48	0.93
1994	-6.38	-0.41	0.9	-5.42	0.67	0.9	-5.77	0.41	0.93
1995	-6.31	-0.78	0.9	-5.38	1	0.9	-5.71	0.32	0.93
1996	-6.14	0.04	0.88	-5.24	0.99	0.93	-5.59	0.6	0.94
1997	-6.55	-0.05	0.9	-5.18	0.64	0.92	-5.71	0.43	0.93
1998	-6.39	-0.28	0.91	-4.91	0.69	0.91	-5.5	0.34	0.94
1999	-6.68	-0.14	0.91	-4.95	0.92	0.93	-5.69	0.53	0.95
2000	-6.14	-0.24	0.93	-4.5	0.6	0.89	-5.23	0.34	0.94
2001	-5.72	-1.04	0.87	-4.27	0.2	0.82	-4.99	-0.17	0.92
2002	-6.38	-0.12	0.91	-4.5	0.71	0.89	-5.32	0.42	0.93
2003	-6.15	-0.04	0.93	-4.12	0.49	0.9	-5.03	0.37	0.95
2004	-6.32	-0.03	0.91	-4.48	0.57	0.9	-5.26	0.41	0.92
2005	-6.25	-0.38	0.93	-4.33	0.35	0.9	-5.18	0.18	0.94
2006	-6.09	-0.23	0.88	-4.44	0.27	0.88	-5.15	0.24	0.91
Average	**-6.05**	**-0.50**	**0.89**	**-4.62**	**0.54**	**0.89**	**-5.26**	**0.23**	**0.93**
STDEV	**0.49**	**0.38**	**0.03**	**0.47**	**0.24**	**0.03**	**0.38**	**0.23**	**0.02**
All Years Regression (Fig. A-2)	**-6.2**	**-0.99**	**0.97**	**-4.63**	**-0.07**	**0.94**	**-5.24**	**-0.3**	**0.97**

(Return to Content)

A-1. Downscaling Methodology

Figure A-2 illustrates the linear dependence of the bias between the GEOS-4 temperatures and elevation differences between reanalysis grid cell and the ground site elevation. In this section a mathematical procedure is developed for statistically calibrating the GEOS-4 model relative to ground site observations resulting parameters that allow downscaled estimates of the reanalysis temperatures at localized ground sites site values. In subsequent sections the validity of the downscaling approach will demonstrated.

The downscaling approach discussed in this appendix is not currently available through the POWER/Agroclimatology archive, and is discussed here only to give a user guidance in its application.

If we assume that the reanalysis modeled temperatures estimates can in fact be downscaled based upon a lapse rate correction, then we can express the downscaled temperatures at a local ground site as

Eq. A-1. $(T^{grd})_{RA} = (T^{nat})_{RA} + \lambda*(H_{grd} - H_{RA}) + \beta$

Where $(T^{grd})_{RA}$ is the downscaled reanalysis temperature, $(T^{nat})_{RA}$ is the native reanalysis value averaged over the reanalysis grid cell, λ is the seasonal/regional lapse rate (C/km) appropriate for the given ground site, H_{grd} and H_{RA} are the elevation for ground site and reanalysis grid cell respectively, and β is included to account for possible biases between the reanalysis model estimates and ground observations. Assuming that Eq. A-1 provides an accurate estimate of the air temperature we have

Eq. A-2. $(T^{grd}) = (T^{grd})_{RA}$,

where (T^{grd}) is the air temperature at the desired ground site.

Equation Eq. A-1 and Eq. A-2 can be combined to yield

Eq. A-3. $(T^{grd}) = (T^{nat})_{RA} + \lambda*(H_{grd} - H_{RA}) + \beta$

or

Eq. A-4. $\Delta T = \lambda*\Delta H + \beta$

where ΔT is the differences between the air temperature at desired ground site and reanalysis cell temperature or Bias, and ΔH is the difference between the elevation of the ground site and the model cell. Equation Eq. A-4 gives a linear relation between ΔT and ΔH with the slope given by λ, the lapse rate, and an intercept value given by β. A linear least squares fit to a scatter plot of ΔT vs ΔH (i.e. Figure A-2) yields λ, the lapse rate, and β, the model bias. These parameters can then be used to downscale the reanalysis temperature values to any ground site within a region that the λ and β values are valid. Note that this methodology lends itself to generating λ and β values averaged over any arbitrary time period and/or investigating other environmental factors such as the influence of the vegetation type on the downscaling methodology.

The scatter plots shown in Figure A-2 are constructed using the yearly mean bias between GEOS-4 and NCEI temperatures (i.e. ΔT) vs the difference in the elevation between the GEOS-4 grid cell and the ground site (i.e. ΔH). Consequently, from Eq. A-4 the slope and intercept associated with the linear fit to the scatter plot give a set of globally averaged λ and β parameters for downscaling the reanalysis temperatures Tave, Tmin, and Tmax to any geographical site. Table A-2 summarizes the values for λ (e.g. lapse rate) and β (e.g. offset) based upon the use of the NCEI GSOD meteorological data as the "calibration" source. The values given in Table A.2 are based upon the globally distributed ground sites in the NCEI GSOD data base, and are based upon yearly mean ground and GEOS-4 data.

Table A-2. Globally and yearly and averaged lapse rate and offset values for adjusting GEOS-4 temperatures to local ground site values (based upon 1983 – 2006 NCEI and GEOS-4 global data).		
	Lapse Rate (^{o}C/km)	Off Set (^{o}C)
Tmax	-6.20	-0.99
Tmin	-4.63	-0.07
Tave	-5.24	-0.30

Figure A-3 illustrates that bias between the ground observations and the GEOS-4 values after applying the lapse rate correction and offset values given in Table A-2 is independent of the elevation difference between the ground site and the GEOS-4 1-degree cell and that the average bias is also near zero.

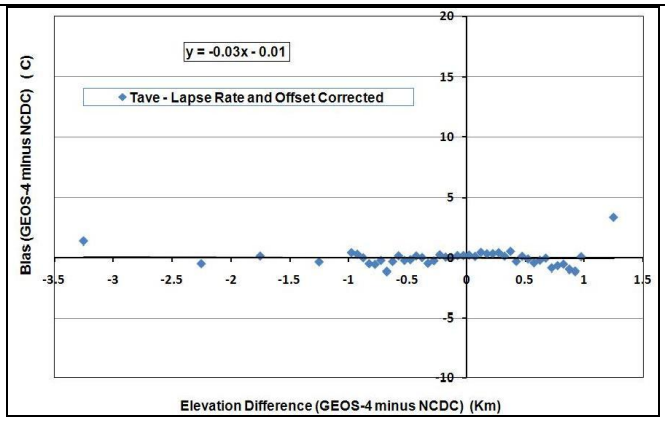

(a)

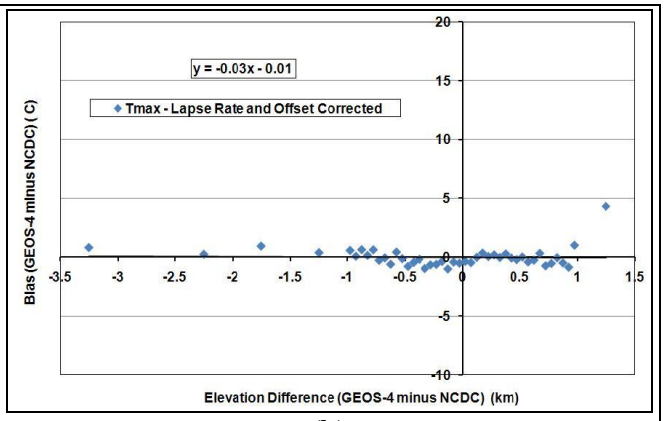

(b)

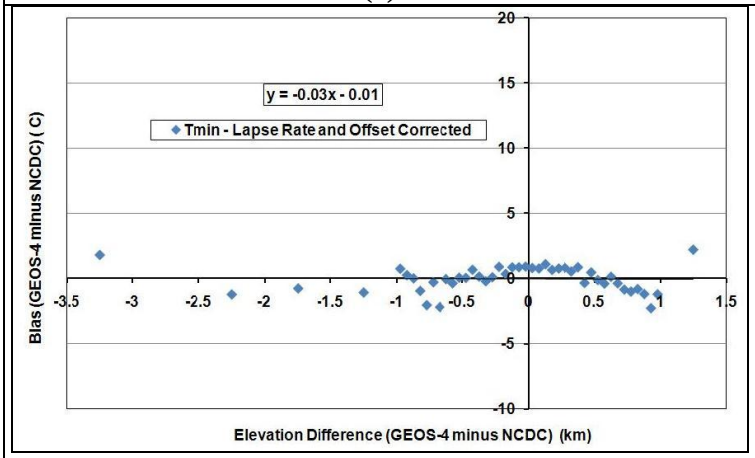

(c)

Figure A-3. Scatter plots showing the dependence of the bias between the GEOS-4 Tave (a), Tmin (b), and Tmax (c) temperatures and values from the NCEI archive on the elevation difference between the GEOS-4 cell and the ground station elevation for the years 1983 -2006 after adjusting the GEOS-4 values using Eq. VII – 3. The elevation difference between stations are grouped into elevation difference bins (e.g. 0 to 50m; >50m to 100m; >100m to 150m; etc.) and plotted against the mean bias for the respective elevation bin.

(Return to Content)

A.ii Global Downscaling: Table A-3 gives the yearly mean global MBE and RMSE of the un-corrected and downscaled GEOS-4 temperature values relative to NCEI values for the year 2007. The 2007 GEOS-4 values were downscaled via Eq. A-3 using the lapse rate and offset parameters given in Table A-2. Since the λ and β parameters for downscaling were developed using NCEI data over the years 1983 – 2006, the use of data from 2007 serves as an independent data set for this test.

Table A-3. Globally and yearly averaged Mean Bias Error (MBE) and Root Mean Square Error (RMSE) for 2007 un-corrected and downscaled GEOS-4 temperatures relative to NCEI temperatures. The downscaled GEOS-4 values are based upon the downscaling parameters given in Table A-2 .

		Un-corrected GEOS-4	Downscaled GEOS-4
Tmax	**MBE**	-1.58	-0.10
	RMSE	3.79	3.17
Tmin	**MBE**	0.27	0.71
	RMSE	3.57	3.42
Tave	**MBE**	-0.50	0.22
	RMSE	2.82	2.47

Note that the lapse rates and offset values given in Table A-2 are yearly averaged values based upon globally distributed ground sites in the NCEI data base. Results from a number of studies have indicated that tropospheric lapse rates can be seasonally and regionally dependent. Table A-4 gives the globally and monthly averaged lapse rate and offset downscaling parameters for GEOS-4 temperatures. These parameters were developed from eq. Eq. A-4 using the monthly averaged temperature data over the years 1983 – 2006 in global distribution of GEOS-4 and NCEI. Tables A-5 and A-6 give respectively the globally and monthly averaged MBE and RMSE of the 2007 GEOS-4 temperatures relative to NCEI ground site values for the unadjusted and downscaled respectively.

Table A-4. Globally and monthly averaged lapse rates and offset values for adjusting GEOS-4 temperatures to local ground site values. Based upon 1983 – 2006 NCEI and GEOS-4 global data.

	JAN	FEB	MAR	APR	MAY	JUN	JUL	AUG	SEP	OCT	NOV	DEC	YR
Tmx λ	-5.12	-5.97	-6.73	-7.2	-7.14	-6.78	-6.52	-6.44	-6.31	-5.91	-5.44	-4.85	-6.22
Tmx β	-1.61	-1.57	-1.4	-1.01	-0.56	-0.29	-0.24	-0.46	-0.67	-1.08	-1.44	-1.55	-0.99
Tmn λ	-4.34	-4.89	-5.17	-5.16	-4.93	-4.67	-4.46	-4.33	-4.28	-4.31	-4.6	-4.44	-4.63
Tmn β	-0.96	-0.95	-0.69	-0.14	0.22	0.34	0.43	0.5	0.58	0.42	-0.06	-0.61	-0.07
Tm λ	-4.49	-5.19	-5.73	-6.06	-5.91	-5.59	-5.35	-5.27	-5.14	-4.9	-4.8	-4.45	-5.24
Tm β	-1.16	-1.09	-0.9	-0.34	0.17	0.42	0.51	0.35	0.13	-0.18	-0.61	-0.97	-0.3

Table A-5. Globally and monthly averaged MBE and RMSE values associated with unadjusted 2007 GEOS-4 temperatures relative to 2007 NCEI GSOD temperatures.

	JAN	FEB	MAR	APR	MAY	JUN	JUL	AUG	SEP	OCT	NOV	DEC	YR
Tmax MBE	-2.00	-2.11	-2.00	-1.64	-1.13	-1.15	-0.84	-1.27	-1.49	-1.85	-1.73	-1.90	-1.89
Tmax RMSE	4.04	4.00	4.01	3.75	3.73	3.64	3.57	3.64	3.66	3.72	3.71	4.02	3.79
Tmin MBE	-0.24	-0.49	-0.23	0.19	0.56	0.49	0.66	0.61	0.81	0.76	0.50	-0.41	0.27
Tmin RMSE	4.13	4.02	3.70	3.32	3.25	3.09	3.10	3.13	3.30	3.50	3.84	4.26	3.55
Tave MBE	-1.0	-1.15	-0.88	-0.54	-0.03	-0.06	-0.13	-0.18	-0.15	-0.43	-0.59	-1.08	-0.50
Tave RMSE	3.20	3.18	2.92	2.62	2.66	2.54	2.55	2.50	2.51	2.56	2.91	3.41	2.80

Table A-6. Globally averaged monthly MBE and RMSE associated with downscaled 2007 temperatures relative to 2007 NCEI GSOD temperatures. The GEOS-4 temperatures were downscaled using the globally and monthly averaged λ and β values given in Table A-4.

	JAN	FEB	MAR	APR	MAY	JUN	JUL	AUG	SEP	OCT	NOV	DEC	YR
Tmax MBE	**0.04**	**-0.07**	**-0.04**	**-0.06**	**0.00**	**-0.32**	**-0.08**	**-0.30**	**-0.32**	**-0.29**	**0.14**	**0.04**	**-0.10**
Tmax RMSE	**3.35**	**3.11**	**3.17**	**2.97**	**3.18**	**3.16**	**3.18**	**3.13**	**3.02**	**2.98**	**3.06**	**3.40**	**3.14**
Tmin MBE	**1.06**	**0.85**	**0.87**	**0.74**	**0.74**	**0.52**	**0.59**	**0.45**	**0.57**	**0.69**	**0.92**	**0.56**	**0.71**
Tmin RMSE	**4.11**	**3.87**	**3.54**	**3.13**	**2.99**	**2.83**	**2.86**	**2.87**	**3.01**	**3.26**	**3.71**	**4.12**	**3.36**
Tave MBE	**0.52**	**0.33**	**0.48**	**0.28**	**0.27**	**-0.04**	**0.04**	**-0.11**	**0.13**	**0.14**	**0.41**	**0.25**	**0.22**
Tave RMSE	**2.94**	**2.69**	**2.44**	**2.11**	**2.22**	**2.18**	**2.24**	**2.16**	**2.12**	**2.20**	**2.61**	**3.06**	**2.41**

(Return to Content)

A.ii. Regional Downscaling: Eq. A-4 can also be used to develop regional specific λ and β values which, for some applications, may be more appropriate than the yearly (Table A-3) or monthly and globally averaged (Table A-4) values. As an example, Table A-7 gives the regionally and monthly averaged λ and β values for Tmax, Tmin, and Tave along with the regionally yearly averaged values for the Pacific Northwest region (40 - 50N, 125 – 110W). These values were developed via Eq. 4 for the US Pacific Northwest using GEOS-4 and NCEI GSOD temperatures over the years from 1983 through 2006.

Table A-7. Regional and monthly averaged lapse rate and offset values for adjusting GEOS-4 temperatures to local ground site values Based upon 1983 – 2006 NCEI and GEOS-4 temperatures in the US Pacific Northwest region.

	JAN	FEB	MAR	APR	MAY	JUN	JUL	AUG	SEP	OCT	NOV	DEC	YR
Tmx λ	-5.13	-6.22	-7.54	-7.88	-7.09	-6.61	-6.29	-5.87	-6.09	-5.83	-5.56	-4.69	-6.23
Tmx β	-1.47	-1.69	-1.63	-1.55	-1.23	-1.12	-1.03	-1.64	-1.82	-2.15	-1.74	-1.09	-1.51
Tmn λ	-5.55	-6.46	-6.68	-6.06	-5.53	-5.64	-5.25	-4.77	-4.7	-4.64	-5.54	-5.37	-5.51
Tmn β	-0.9	-0.69	-0.12	0.31	0.48	0.78	1.36	1.43	1.31	0.81	0.31	-0.68	0.37
Tm λ	-5.35	-6.38	-7.11	-7.26	-6.55	-6.27	-5.87	-5.54	-5.58	-5.39	-5.55	-5.02	-5.98
Tm β	-0.81	-0.7	-0.48	-0.06	0.4	0.7	0.97	0.58	0.2	-0.19	-0.32	-0.61	-0.02

The MBE and RMSE of the unadjusted 2007 GEOS-4 temperatures in the US Pacific Region relative to the ground observations are given in Table A-8, and for comparison the MBE and RMSE associated with the downscaled 2007 GEOS-4 temperatures are given in Table A-9. The downscaled temperatures are based upon Eq. 3 using the regional λ and β values given in Table 7.

Table A-8. Regional monthly MBE and RMSE values associated with unadjusted 2007 GEOS-4 temperatures in the US Pacific region relative to 2007 NCEI GSOD temperatures

	JAN	FEB	MAR	APR	MAY	JUN	JUL	AUG	SEP	OCT	NOV	DEC	YR
Tmax MBE	-3.05	-3.41	-4.47	-3.96	-3.10	-3.47	-2.74	-3.23	-3.58	-3.77	-3.25	-3.18	-3.43
Tmax RMSE	5.06	5.11	5.78	5.34	5.06	5.18	4.85	5.28	5.63	5.36	4.99	4.76	5.20
Tmin MBE	-2.59	-2.90	-2.85	-2.30	-1.51	-1.50	-0.34	-0.12	-0.39	-1.19	-1.40	-2.94	-1.67
Tmin RMSE	5.58	5.32	5.03	4.45	4.18	4.36	4.25	4.22	4.33	3.95	4.71	5.53	4.66
Tave MBE	-2.40	-2.56	-3.12	-2.59	-1.52	-1.65	-0.83	-1.15	-1.54	-1.99	-2.11	-2.79	-2.02
Tave RMSE	4.36	4.12	4.33	3.92	3.33	3.38	3.16	3.21	3.41	3.48	3.92	4.52	3.76

Table A-9. Regional monthly MBE and RMSE values associated with downscaled 2007 GEOS-4 temperatures in the US Pacific region relative to 2007 NCEI GSOD temperatures. The GEOS-4 temperatures were downscaled using the regionally and monthly averaged λ and β values for the US pacific Region given in Table A-7.

	JAN	FEB	MAR	APR	MAY	JUN	JUL	AUG	SEP	OCT	NOV	DEC	YR
Tmax MBE	**0.28**	**0.54**	**-0.11**	**0.45**	**0.70**	**0.05**	**0.58**	**0.54**	**0.45**	**0.50**	**0.51**	**-0.39**	**0.34**
Tmax RMSE	**4.00**	**3.63**	**3.45**	**3.11**	**3.77**	**3.55**	**3.90**	**4.05**	**4.21**	**3.70**	**3.71**	**3.30**	**3.70**
Tmin MBE	**0.32**	**0.14**	**-0.32**	**-0.41**	**0.01**	**-0.23**	**0.20**	**0.18**	**0.00**	**-0.31**	**0.30**	**-0.32**	**-0.04**
Tmin RMSE	**4.58**	**3.96**	**3.62**	**3.25**	**3.38**	**3.49**	**3.70**	**3.71**	**3.88**	**3.41**	**4.05**	**4.31**	**3.78**
Tave MBE	**0.35**	**0.46**	**-0.07**	**0.10**	**0.46**	**-0.08**	**0.33**	**0.28**	**0.28**	**0.15**	**0.22**	**-0.36**	**0.18**
Tave RMSE	**3.41**	**2.81**	**2.42**	**2.09**	**2.36**	**2.32**	**2.58**	**2.47**	**2.49**	**2.45**	**2.91**	**3.25**	**2.63**

As an additional point of comparison Table A-10 gives the MBE and RMSE values associated with downscaled 2007 GEOS-4 temperatures in the US Pacific Northwest relative to 2007 NCEI GSOD temperatures where the globally and monthly averaged (Table 4) downscaling parameters (i.e. λ and β) have used.

Table A-10. MBE and RMSE associated with downscaled 2007 temperatures relative to 2007 NCEI GSOD temperatures in the US Pacific Northwest region (40 – 50N, 125 – 110W). The GEOS-4 temperatures were downscaled using the globally and monthly averaged λ and β values given in Table A.6

	JAN	FEB	MAR	APR	MAY	JUN	JUL	AUG	SEP	OCT	NOV	DEC	YR
Tmax MBE	0.42	0.33	-0.63	-0.33	0.05	-0.72	-0.13	-0.43	-0.63	-0.54	0.16	0.13	-0.19
Tmax RMSE	4.02	3.60	3.48	3.08	3.71	3.62	3.86	4.05	4.24	3.71	3.67	3.28	3.69
Tmin MBE	-0.06	-0.17	-0.29	-0.29	0.05	-0.15	0.85	0.95	0.58	-0.04	0.33	-0.72	0.09
Tmin RMSE	4.61	4.02	3.67	3.28	3.41	3.55	3.85	3.85	3.95	3.41	4.10	4.40	3.84
Tave MBE	0.39	0.42	-0.15	-0.05	0.45	-0.05	0.60	0.41	0.20	-0.03	0.24	-0.20	0.18
Tave RMSE	3.42	2.82	2.44	2.13	2.37	2.34	2.64	2.50	2.50	2.45	2.93	3.25	2.65

The monthly time series of MBE and RMSE values for GEOS-4 2007 temperatures relative to NCEI ground site values provide a summary for the un-scaled and downscaled temperatures in the US Pacific Northwest region. The 2007 downscaled GEOS-4 temperatures are based upon the monthly averaged λ and β values developed from 1983 – 2006 GEOS-4 and NCEI data in this region. The MBE and RMSE monthly time series values are plotted for the uncorrected GEOS-4 and GEOS-4 downscaled using (1) yearly and global mean lapse rate and offset values, (2) monthly mean global lapse rate and offset values, (3) yearly mean regional lapse rate and offset values, and (4) monthly mean regional lapse rate and offset values.

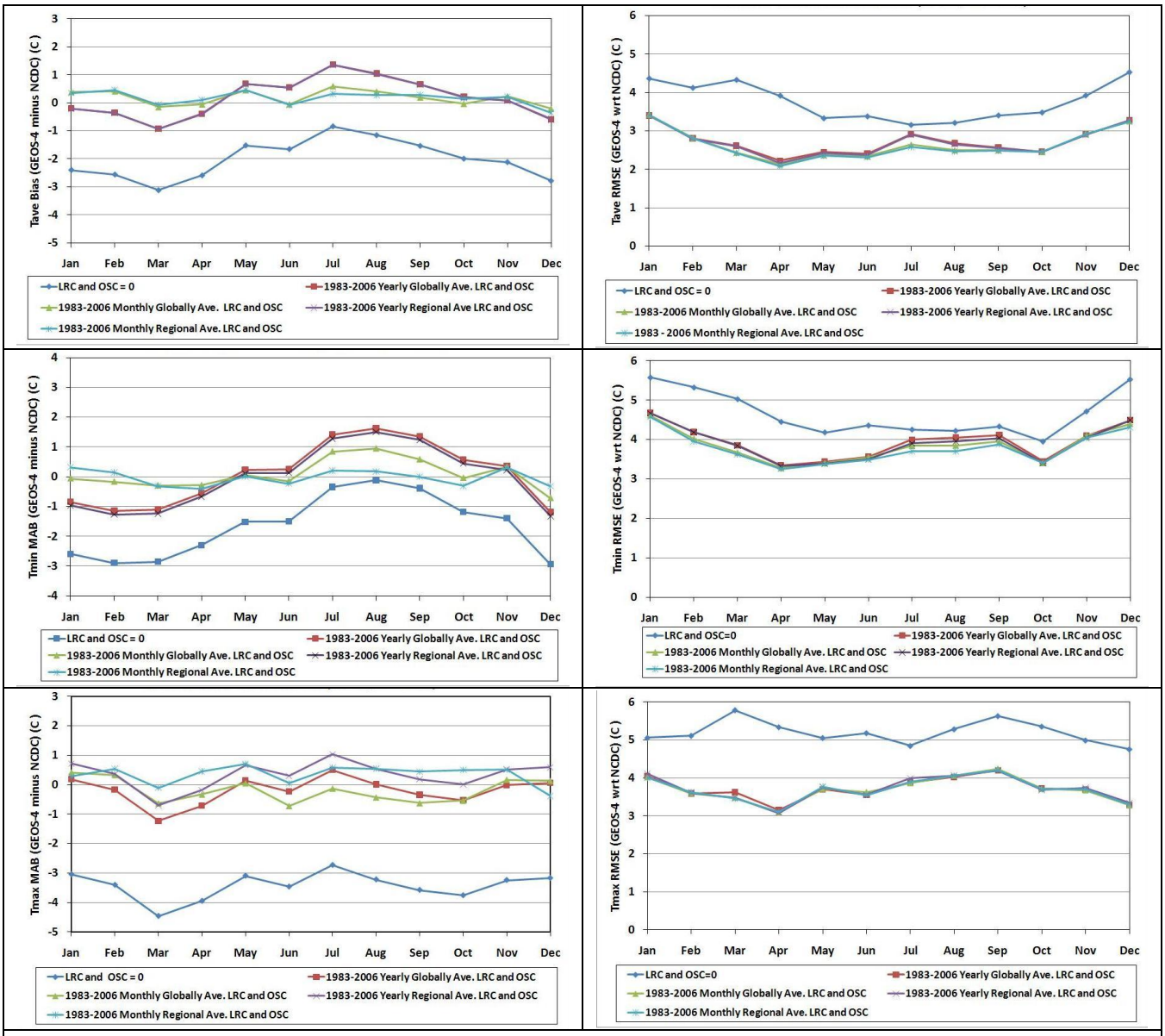

Figures A-4. Monthly time series of the MBE (left column) and RMSE (right column) between 2007 un-scaled and downscaled GEOS-4 and NCEI ground sites observations in the Pacific Northwest region (40 - 50N, 125 – 110W). The MBE and RMSE monthly time series values are plotted for the (1) uncorrected GEOS-4 (i.e. LRC and OSC = 0) and GEOS-4 corrected using (2) yearly and global mean lapse rate and offset values, (3) monthly mean global lapse rate and offset values, (4) yearly mean regional lapse rate and offset values, and (5) monthly mean regional lapse rate and offset values. The downscaling parameters are based upon GEOS-4 and NCEI station temperatures over the years 1983 – 2006.

For each set of downscaling parameters (i.e. lapse rate and offset) there is a substantial reduction in the MBE and RMSE relative to the un-adjusted GEOS-4 values; however, there is little difference in the downscaled RMSE values relative to the temporal averaging period (i.e. yearly vs. monthly average) or geographical region (global vs. regional) used to generate the downscaling parameters. The MBE is, however somewhat more dependent on the set of downscaling parameters, with the monthly mean regional values yielding the lowest MBE errors, particularly in the MBE for Tmin.

The downscaling discussed in this appendix is not currently available through the POWER/Agroclimatology archive, and is discussed here only to give users guidance in its application.

(Return to Content)